American Mineralogist, Volume 97, pages 2007–2015, 2012

Whelanite, $Cu_2Ca_6[Si_6O_{17}(OH)](CO_3)(OH)_3(H_2O)_2$, an (old) new mineral from the Bawana mine, Milford, Utah

Anthony R. Kampf,[1,*] Stuart J. Mills,[2] Stefano Merlino,[3] Marco Pasero,[3] Andrew M. McDonald,[4] William B. Wray,[5] and James R. Hindman[6]

[1]Mineral Sciences Department, Natural History Museum of Los Angeles County, 900 Exposition Boulevard, Los Angeles, California 90007, U.S.A.
[2]Geosciences, Museum Victoria, GPO Box 666, Melbourne 3001, Australia
[3]Dipartimento di Scienze della Terra, Università di Pisa, Via S. Maria 53, 56126 Pisa, Italy
[4]Department of Earth Sciences, Laurentian University, Sudbury, Ontario P3E 2C6, Canada
[5]2700 Las Vegas Boulevard South, no. 3310, Las Vegas, Nevada 89109, U.S.A.
[6]715 East Glendale Street, Dillon, Montana 59725, U.S.A.

Abstract

The new mineral whelanite, $Cu_2Ca_6[Si_6O_{17}(OH)](CO_3)(OH)_3(H_2O)_2$, was approved by the Commission on New Minerals and Mineral Names (IMA) in 1977, but until now a description has not been published. The mineral is orthorhombic with space group *Pn*2*n* and cell parameters $a = 5.6551(4)$, $b = 3.683(3)$, $c = 27.1372(7)$ Å, $V = 565.3(5)$ Å^3, and $Z = 1$. The mineral occurs with thaumasite, stringhamite, and kinoite in a copper-rich, diopside–garnet–magnetite skarn at the Bawana mine, Beaver County, Utah, and has also been confirmed to occur at other localities. At the Bawana mine, it is found as irregular clusters and radial aggregates of platy to lath-like crystals up to 1 mm in length, flattened on {001} and elongated on [100]. The color and streak are pale blue and the luster is vitreous. The laths are flexible, but not elastic. Cleavage is perfect on {001} and good on {010}, producing splintery fracture. The Mohs' hardness is about 2½. The measured density is 2.74(3) g/cm^3 and the calculated density is 2.737 g/cm^3 based upon the empirical formula. The mineral is biaxial (–), $\alpha = 1.612(2)$, $\beta = 1.622$(calc), and $\gamma = 1.626(2)$, and $2V_{meas} = 64(1)°$. The pleochroism is weak: X = Y (pale blue) < Z (light blue). The optical orientation is X = **a**, Y = **c**, Z = **b**. A combination of electron microprobe analyses and thermogravimetric analyses (for CO_2 and H_2O) yielded: CaO 34.46, CuO 12.09, FeO 1.52, SiO_2 37.96, CO_2 5.93, H_2O 8.86, total 100.82 wt%, providing the empirical formula (based on O = 26): $Cu_{1.41}Fe_{0.20}Ca_{5.68}Si_{5.84}C_{1.25}O_{26}H_{9.09}$. Raman spectroscopy shows evidence of $(CO_3)^{2-}$, $(OH)^-$, and H_2O. The strongest powder X-ray diffraction lines are [*d*(*hkl*)*I*]: 6.79(004)52, 3.072(111)43, 3.013(112)100, 2.921(113)39, 2.802(114)45, 2.522(116,205)44, and 1.839(020,1.1.12)37. The crystal structure (R_1 = 3.89% for 567 $F_o > 4\sigma F$) contains two different types of polyhedral layers parallel to {001}, which alternate along [001] and are linked to one another by sharing corners with wollastonite-like silicate chains running parallel [010]. One polyhedral layer, consisting of edge-sharing CaO_7 polyhedra, is identical to that in the structures of the tobermorites (tobermorite 9Å, tobermorite 11Å, tobermorite 14Å, and clinotobermorite). The other layer is brucite-like, with alternating ribbons of edge-sharing $Cu^{2+}O_6$ and CaO_6 octahedra. Disordered CO_3 and H_2O groups are also located in the interlayer region. The crystal structure of whelanite exhibits OD character.

Keywords: Whelanite, new mineral, crystal structure, order-disorder structure, Raman spectroscopy, Bawana mine, Milford, Utah

Introduction

The proposal for the new mineral whelanite (phonetically pronounced: WEE-lan-ite), submitted by one of the authors (J.R.H.), was approved by the Commission on New Minerals and Mineral Names (now known as the Commission on New Minerals, Nomenclature and Classification) of the International Mineralogical Association in 1977; however, until now, no formal description of the mineral has been published. A major stumbling block in investigations of the mineral has been the solution of its structure, which has proven quite elusive because of the thinness and generally poor quality of the vast majority of crystals, but more importantly, the disorder affecting the silicate-carbonate interlayer portion of the structure.

As indicated in the new mineral abstract, IMA 1977-006, type material is preserved in the Smithsonian Institution (U.S. National Museum of Natural History) and the Los Angeles County Museum of Natural History (now known as the Natural History Museum of Los Angeles County). The formal description of whelanite, provided herein, is based in part on data from the original study (density and TGA), but mostly on new data obtained from co-type material (10 specimens) in the Natural History Museum of Los Angeles County under catalog numbers 15507–15516.

* E-mail: akampf@nhm.org

0003-004X/12/1112–2007$05.00/DOI: http://dx.doi.org/10.2138/am.2012.4181

The mineral name honors the late James A. Whelan (1928–2003), who was a professor of mineralogy at the University of Utah, where he taught from 1958 to 1992.

Occurrence

The original specimens of whelanite were collected in 1969 at the Bawana (open pit) copper–magnetite mine, located about 5 miles NW of Milford in the Rocky mining district, Beaver County, Utah. The Bawana deposit, originally covered under several tens of feet of alluvium, was discovered by drilling a ground magnetic anomaly in late 1956, and was mined as an open pit from 1962 to 1967 (Wray 2006). A discussion of the geology and mineralogy of the area was provided by Hintze and Whelan (1973), and more recently by Wray (2006). We have also confirmed whelanite to occur on specimens from the Christmas mine, Pinal County, Arizona, and the Sunrise copper prospect near Bird Springs in the Nelson Range, Inyo County, California. A mineral from the Crestmore quarry, Riverside County, California, originally referred to by Murdoch (1961) as "mineral Y", appears to be closely related to whelanite. Numerous single-crystal samples of mineral Y that we examined provided powder X-ray diffraction patterns consistent with varying mixtures of whelanite and tobermorite 14Å, suggesting that the structure of this mineral may consist of interstratified whelanite and tobermorite 14Å layers.

At all of the localities whelanite is found as a late-stage phase in copper-rich, calc-silicate skarn assembages. At the Bawana mine, the mineral occurs with kinoite, stringhamite (Hindman 1976) and thaumasite on rock containing diopside, garnet (grossular–andradite), goethite, magnetite, and tenorite. Chrysocolla (including a blue copper-bearing silica gel) is abundant in the deposit and may occur on or near specimens containing whelanite and/or stringhamite. At the Christmas mine, whelanite occurs with gilalite, ruizite, stringhamite, and tobermorite 11Å on rock containing andradite, bornite, calcite, chalcopyrite, quartz, and wollastonite. At the Sunrise prospect, it occurs with apophyllite, lepidocrocite, stringhamite, and thaumasite on rock containing bornite, calcite, diopside, grossular, and tenorite. At the Crestmore quarry, the whelanite-like mineral occurs with foshagite, ganomalite, stringhamite, thaumasite, and tobermorite 14Å on rock containing calcite, galena, grossular, vesuvianite, and wollastonite.

The Rocky mining district contains other oxidized, near-surface copper–magnetite skarn deposits, several of which (the Maria, Hidden Treasure, and Hidden Treasure NW Extension deposits, in particular) have been mined. Despite efforts to locate whelanite in ore from these nearby, similar deposits, none has been found. Of possible significance is that these other deposits appear to lack the particular grossular–andradite host-rock association seen with the whelanite (and stringhamite) in the Bawana deposit. It is also noteworthy that mcguinnessite, which is similar in appearance to whelanite, occurs in small amounts as thin veinlets in massive magnetite in skarns of the Maria, Hidden Treasure, and Hidden Treasure NW Extension deposits, but has never been recognized in the Bawana deposit. Other oxidized copper-bearing skarn mines and deposits in the district, including among others the Old Hickory, Niagara, Sunrise, and Copper Ranch, are not known to contain any whelanite, stringhamite, or mcguinnessite.

After mining ceased at the Bawana mine, whelanite and associated stringhamite were only found within a small area of skarn rubble near the midpoint of the bottom of the open pit. Several decades of mineral collecting has depleted the occurrence, and recent excavation activity by a mining company has further disturbed the pit bottom, such that at the present time it is difficult or impossible to find specimens of these minerals.

Physical and optical properties

At the Bawana mine (and at the other localities), whelanite is found as irregular clusters and radial aggregates of platy to lath-like crystals (Figs. 1 and 2) up to 1 mm in length, flattened on {001} and elongated on [100]. Because of the thinness of the crystals, bounding forms could not be measured; however, based upon the shape of the laths, the {010} form accounts for the long edges of the laths and the terminations can be one of several {*hk*0} forms: {210}, {110}, {120}, or {130} (Fig. 3). The color and streak are pale blue and the luster is vitreous. The laths are flexible, but not elastic. Cleavage is perfect on {001} and good on {010}, producing splintery fracture. The Mohs hardness is about 2½. The measured density is 2.74(3) g/cm^3. The calculated density based upon the empirical formula and single-crystal cell is 2.738 g/cm^3 and that based upon the ideal formula is 2.856 g/cm^3.

Owing to the thinness of the plates, the β optical constant

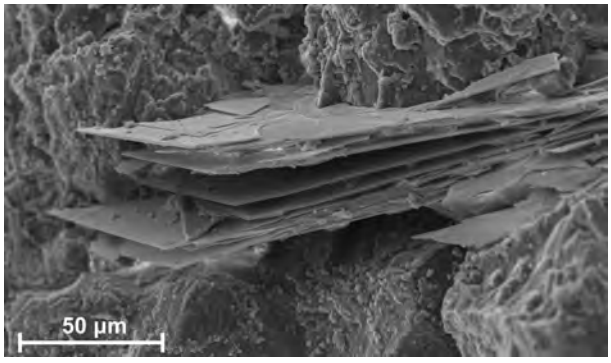

Figure 1. SEM image of whelanite from the Bawana mine.

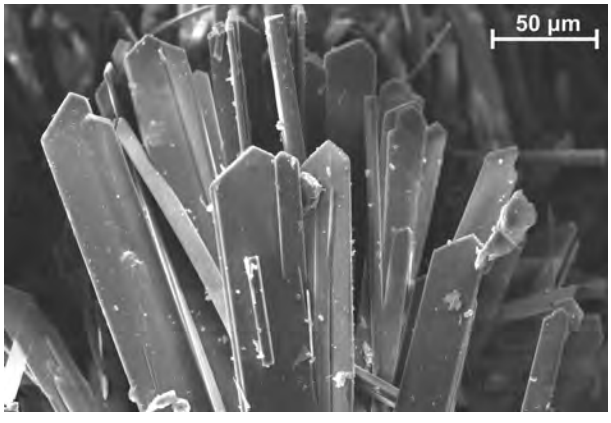

Figure 2. SEM image of whelanite from the Sunshine copper prospect.

could not be measured, and because of the unfavorable orientation, the interference figure could not be directly observed. Extinction data obtained on a Supper spindle stage were used with the program EXCALIBRW (Gunter et al. 2004) to determine the $2V$ angle. From the $2V$ and the measured indices of refraction α and γ, the value of β was calculated. All optical data were obtained in white light. Whelanite is optically biaxial (–) with optical constants: $\alpha = 1.612(2)$, $\beta = 1.622$(calc), and $\gamma = 1.626(2)$, and $2V_{meas} = 64(1)°$. The pleochroism is weak: $X = Y$ (pale blue) $< Z$ (light blue). The optical orientation is $X =$ **a**, $Y =$ **c**, $Z =$ **b**.

The Gladstone-Dale compatibility index $1 - (K_P/K_C)$, as defined by Mandarino (1981), is –0.037, indicating excellent agreement among the average index of refraction, calculated density, and chemical composition.

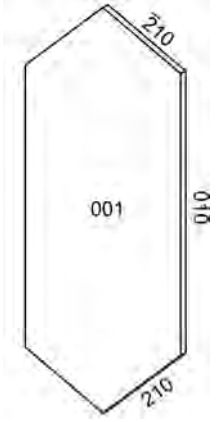

FIGURE 3. Crystal drawing of whelanite (clinographic projection in non-standard orientation).

RAMAN SPECTROSCOPY

Owing to questions regarding the chemical species present in whelanite, a Raman spectroscopic study was undertaken in this study. Subsequent to this, a published Raman spectrum of the mineral, obtained on non-type material from the Christmas mine, Gila Co., Arizona, was discovered (Frost and Xi 2012). Ignoring differences in band assignments and the number of peaks fit to some of the broader peaks, the two spectra are quite comparable in terms of the peaks present and their relative intensities. Given the similarity between the two spectra and that the current one was collected on type material, only the Raman spectrum from the Bawana mine (this study) is presented. The Raman spectrum (average of three, 30 s spectra) of a single crystal of whelanite was obtained over the range of 50 to 4000 cm^{-1} (Fig. 4). Data were collected in backscattered mode with a HORIBA Jobin Yvon XploRA spectrometer interfaced with an Olympus BX 41 microscope, 100× magnification (estimated spot size of 2 μm), a 1200 grating and an excitation radiation of 532 nm. Calibration was made using the 521 cm^{-1} line of Si from a silicon wafer. The Raman spectrum is dominated by a relatively sharp band at 671 cm^{-1} (weak shoulder at 715 cm^{-1}; attributable to asymmetrical Si-O bending, υ_4) that, along with several others below 1100 cm^{-1}, confirm the presence of SiO_4 in the mineral. The spectrum also shows strong peaks at 3558 cm^{-1} (shoulder at 3599 cm^{-1}) and 2954 cm^{-1} (shoulder at 2917 cm^{-1}) that can be

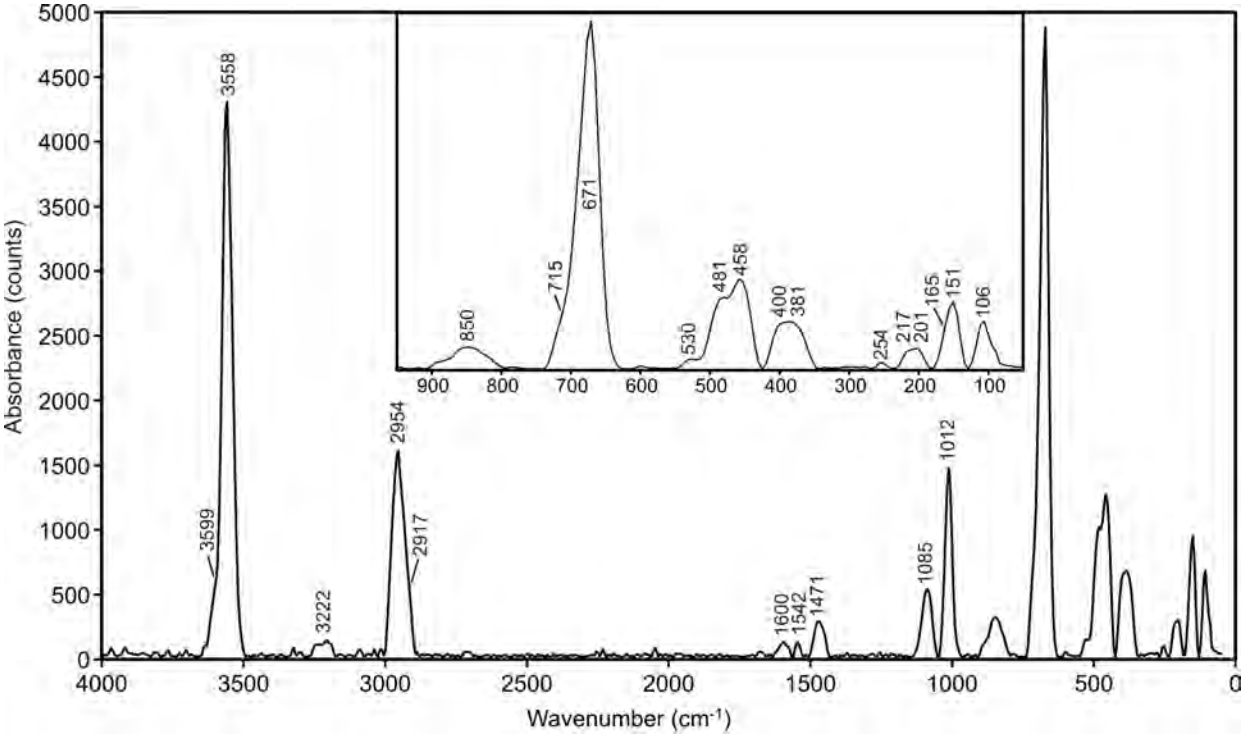

FIGURE 4. Raman spectrum for whelanite from 4000 to 50 cm^{-1}. Inset shows an expanded view of the region from 950 to 50 cm^{-1}. The absorption peaks are labeled with wavenumbers.

attributed to O-H stretching. Some Raman studies have argued that for multiple peaks in the region of 3000–3500 cm^{-1}, bands at relatively high frequencies are attributable to $(OH)^-$ and those at lower ones to H_2O [e.g., kovdorskite, $Mg_2PO_4(OH)\cdot 3H_2O$; Morrison et al. 2012]. In light of this, those bands near 3500 cm^{-1} could correspond to O-H stretching in $(OH)^-$ groups and those near 3000 cm^{-1} to that in H_2O groups. Thus the two sets of O-H stretching bands are taken as evidence that both species are present in whelanite. The region near 1500 cm^{-1} shows three weak absorption bands, two at 1600 and 1542 cm^{-1} that are attributable to H-O-H bending, thus implying the presence of molecular H_2O and one at 1471 cm^{-1}, attributable to C-O bending, thus confirming the presence of carbonate in the mineral. Table 1 lists all the observed absorption bands and the suggested assignments present in the Raman spectrum of whelanite. It should be noted that there is potential for overlap among several bands and these have been duly noted.

Chemistry

The original study of whelanite included chemical analyses utilizing various methods: electron microprobe (EMPA) for CaO, MgO, and CuO; wet chemical (WCA) for FeO and SiO_2; and thermogravimetric (TGA) for CO_2 and H_2O. In the present study, EMPA data for CaO, CuO, FeO, and SiO_2 (no other elements besides these having been detected) were collected by energy-dispersive spectrometry on a JEOL 6400 scanning electron microscope equipped with an Oxford Instruments INCA energy-dispersive spectrometer, operating at 20 kV with a 1 nA beam, and employing data collection times of 60 s. The system was first optimized for quantitative analyses using the Ni$K\alpha_1$ and Ni$K\alpha_2$ lines from metallic Ni, with chalcopyrite (Cu$K\alpha$, Fe$K\alpha$), quartz (Si$K\alpha$), and fluorite (Ca$K\alpha$) being used as internal standards. Results of the original TGA were used for CO_2 and H_2O. These combined data yield: CaO 34.46, CuO 12.09, FeO 1.52, SiO_2 37.96, CO_2 5.93, H_2O 8.86, total 100.82 wt%, providing the empirical formula (based on O = 26): $Cu_{1.41}Fe_{0.20}Ca_{5.68}Si_{5.84}C_{1.25}O_{26}H_{9.09}$. The ideal formula is $Cu_2Ca_6[Si_6O_{17}(OH)](CO_3)(OH)_3(H_2O)_2$, which requires CaO 34.61, CuO 16.36, SiO_2 37.08, CO_2 4.53, H_2O 7.41, total 100.00 wt%. As noted above, Raman spectroscopy confirms the presence of $(CO_3)^{2-}$ and suggests the presence of both $(OH)^-$ and H_2O.

Table 1. Observed absorption bands (cm^{-1}) and band assignments for the Raman spectrum of whelanite

Band	Strength	Suggested assignment
3599	m	Stretching mode of OH groups
3558	vs	Stretching mode of OH groups
3222	w	Stretching mode of OH groups
2954	s	Stretching mode of H_2O molecules
2917	m	Stretching mode of H_2O molecules
1600	w	H-O-H bend
1542	w	H-O-H bend/C-O Asymmetric stretching mode
1471	w	C-O Asymmetric stretching mode
1085	m	Si-O Asymmetric stretching mode/ C-O Symmetric stretching mode
1012	s	Si-O Asymmetric stretching mode
850	w	Si-O Symmetric stretching mode
715	w	Si-O Asymmetric bending mode/C-O Bending mode
671	vs	Si-O Asymmetric bending mode
530	w	Si-O Asymmetric bending mode
481	m	Si-O Symmetric bending mode
458	m	Si-O Symmetric bending mode
400	m	Cu-O, Ca-O stretching modes
381	m	Cu-O, Ca-O stretching modes
217	w	Lattice vibrations
201	w	Lattice vibrations
151	m	Lattice vibrations
106	m	Lattice vibrations

Note: vs = very strong, m = medium, w = weak.

X-ray crystallography and structure determination

Both powder and single-crystal X-ray diffraction data were obtained on a Rigaku R-Axis Rapid II curved imaging plate microdiffractometer utilizing monochromatized Mo$K\alpha$ radiation. For the powder-diffraction study, a Gandolfi-like motion on the φ and ω axes was used to randomize the sample and observed *d*-spacings and intensities were derived by profile fitting using JADE 2010 software. The powder data presented in Table 2 show good agreement with the pattern calculated from the structure determination.

Previous efforts to obtain single-crystal data had been plagued by severe streaking of diffraction spots due to the occurrence of crystals as fine-scale intergrowths of warped laths. A large number of crystal fragments were examined before one that provided single diffraction spots with minimal streaking was found. Even so, because of the extreme thinness (1 μm) of this blade, diffraction intensity fell off precipitously above 45 °2θ, limiting our data set.

The Rigaku CrystalClear software package was used for processing of the structure data including corrections for Lorentz and polarization effects and the application of an empirical multi-scan absorption correction using ABSCOR (Higashi 2001). The SHELXL-97 software (Sheldrick 2008) was used, with neutral atom scattering factors, for the determination (by direct methods) and refinement of the structure. The location of most atoms in the structure was straightforward in space group *Pn*2*n* with the cell: $a = 5.6551(4)$, $b = 3.683(3)$, and $c = 27.1372(7)$ Å; however, the Si2 site exhibited approximately half occupancy, the Si1 site was split into two sites, each with half occupancy, the geometries of the SiO_4 groups were highly irregular and no straightforward CO_3 group could be located. A variety of alternate unit cells with multiples of the cell dimensions were attempted, along with different space groups ranging even to *P*1, in an effort to establish reasonable SiO_4 (and CO_3) group geometries, but without positive results. We ultimately concluded that the irregular SiO_4 configurations are best explained by recourse to order-disorder (OD) theory, as explained below. The "missing" CO_3 group is not addressed in the OD analysis and we found no definitive evidence for its placement in the structure. In the discussion below, we conjecture on its possible placement; however, it should be noted here that the amount of CO_3 in the empirical formula would require a C site that is only about ¼ occupied, so it is not surprising that the CO_3 group is not clearly resolved in the difference maps.

The structure refinement, based upon the aforementioned space group and cell, represents the average structure. The two Ca sites (Ca1 and Ca2) refine to close to full occupancy, but the Cu site refines to somewhat less than full occupancy. All of the O sites associated with the Cu and Ca polyhedra (O1, O2, O3, O4, and O5) refine to close to full occupancy, while the O sites between the polyhedral layers (O6a, O6b, and O7)

TABLE 2. Observed and calculated X-ray powder-diffraction data for whelanite

I_{obs}	d_{obs}	d_{calc}	I_{calc}	*hkl*	I_{obs}	d_{obs}	d_{calc}	I_{calc}	*hkl*
52	6.79(4)	6.7843	74	0 0 4			2.0379	6	1.1.10
		5.5362	7	1 0 1	15	2.008(7)	2.0093	18	2 1 6
17	5.21(6)	5.2199	31	1 0 2	12	1.947(11)	1.9579	8	2.0.10
32	4.52(2)	4.5229	59	0 0 6			1.9413	8	2 1 7
18	3.65(5)	3.6495	13	0 1 1	10	1.874(7)	1.8709	18	2 1 8
7	3.53(3)	3.5321	21	1 0 6	37	1.839(6)	1.8415	35	0 2 0
28	3.40(5)	3.4111	11	0 1 3			1.8241	30	1.1.12
19	3.22(7)	3.1975	16	1 0 7	9	1.776(7)	1.7772	8	0 2 4
43	3.072(13)	3.0664	51	1 1 1			1.7661	8	2.0.12
100	3.013(16)	3.0093	100	1 1 2	12	1.728(18)	1.7288	12	2.1.10
39	2.921(14)	2.9209	41	1 1 3	8	1.703(19)	1.7056	7	0 2 6
		2.9090	14	1 0 8			1.6953	5	3 0 7
		2.8123	17	2 0 1	28	1.678(5)	1.6780	29	3 1 0
45	2.802(11)	2.8092	46	1 1 4	16	1.649(8)	1.6415	9	1.1.14
		2.7681	12	2 0 2	8	1.628(13)	1.6289	9	3 1 4
54	2.722(21)	2.7137	30	0.0.10	12	1.598(6)	1.5988	7	2.0.14
		2.6828	11	1 1 5			1.5984	8	3 0 9
		2.6607	10	1 0 9	5	1.572(15)	1.5732	5	3 1 6
11	2.609(18)	2.6099	19	2 0 4			1.5559	6	1 2 8
44	2.522(11)	2.5493	30	1 1 6	31	1.525(10)	1.5332	6	2 2 2
		2.5077	17	2 0 5			1.5238	12	0.2.10
		2.4466	6	1.0.10			1.5076	5	0.0.18
12	2.408(18)	2.3976	15	2 0 6			1.5047	5	2 2 4
8	2.333(11)	2.3331	16	0 1 9			1.4864	7	1.1.16
27	2.271(12)	2.2828	31	1 1 8	6	1.461(7)	1.4604	5	2 2 6
		2.2614	5	0.0.12			1.4545	5	2.0.16
		2.2612	5	1.0.11	9	1.427(8)	1.4272	9	3.1.10
13	2.16(9)	2.1719	11	2 0 8	16	1.405(7)	1.4062	9	4 0 2
		2.1567	6	1 1 9			1.4046	5	2 2 8
18	2.135(13)	2.1295	17	2 1 4					

Notes: I_{obs} and d_{obs} derived by profile fitting using JADE 2010 software. I_{calc} and d_{calc} calculated from the crystal structure using JADE 2010. Only calculated lines with intensities of 5 or greater are listed. Unit-cell parameters refined from the powder data using JADE 2010 with whole pattern fitting are: a = 5.6571(15), b = 3.6783(9), and c = 27.141(8) Å.

refine to close to half occupancy. Each of the Si sites (Si1a, Si1b, and Si2) also refine to about half occupancy. In the final refinement, all of the sites were assigned either full or half occupancy, as noted above, except the Cu site, for which the occupancy was refined. Note that the small amount of Fe detected in the chemical analysis does not account for the significant deficiency in scattering for the Cu site. We conclude that the low occupancy for this site reflects a real deficiency in Cu + Fe for the site, as also indicated by the lower than stoichiometric Cu + Fe total in the empirical formula. In the final refinement, we also employed the DFIX command to constrain the Si1a-O7 and Si1b-O7 distances to 1.63(2) Å to yield more normal Si-O bond lengths. We were unsuccessful in constraining the very long Si2-O4 bond (1.84 Å) to a more reasonable length and are forced to conclude that it is an artifact of the structural disorder. We were also unsuccessful in locating the CO_3 group indicated by the chemical analyses and Raman spectroscopy. No configurations of located O atoms and/or electron density residuals appear consistent with a CO_3 group.

The Flack parameter (Flack and Bernardinelli 1999), 0.37(12), indicated the likely presence of merohedral twinning and the TWIN instruction was included in the final refinement, which converged to R_1 = 3.89% for 567 reflections with $F_o > 4\sigma F$. The details of the data collection and structure refinement are provided in Table 3. The final atomic coordinates and displacement parameters are in Table 4. Selected interatomic distances and angles are listed in Table 5 and a bond-valence analysis is provided in Table 6. (CIF and structure factors on deposit[1].)

TABLE 3. Data collection and structure refinement details for whelanite

Diffractometer	Rigaku R-Axis Rapid II
X-ray radiation/power	Mo$K\alpha$ (λ = 0.71075 Å)/50 kV, 40 mA
Temperature	298(2) K
Structural formula (without C and H)	$Cu_{1.86}Ca_6Si_6O_{26}$
Space group	*Pn*2*n*
Unit-cell dimensions (Å)	a = 5.6551(4)
	b = 3.683(3)
	c = 27.1372(7)
Z	1
Volume (Å^3)	565.3(5)
Density (for structural formula) (g/cm^3)	2.771
Absorption coefficient (mm^{-1})	3.552
F(000)	465.9
Crystal size (μm)	150 × 50 × 1
θ range (°)	3.00 to 22.44
Index ranges	$-6 \le h \le 6$, $-3 \le k \le 3$, $-29 \le l \le 29$
Reflections collected/unique	3135/705 [R_{int} = 0.076]
Reflections with $F_o > 4\sigma F$	567
Completeness to θ = 23.25°	98.8%
Max. and min. transmission	0.9965 and 0.6178
Refinement method	Full-matrix least-squares on F^2
Parameters refined	89
GoF	1.069
Final R indices [$F_o > 4\sigma F$]	R_1 = 0.0389, wR_2 = 0.0818
R indices (all data)	R_1 = 0.0553, wR_2 = 0.0898
Flack parameter	0.37(12)
Largest difference peak/hole (e/A^3)	+0.99/–0.43

Notes: $R_{int} = \Sigma|F_o^2 - F_o^2(\text{mean})|/\Sigma[F_o^2]$. GoF = $S = \{\Sigma[w(F_o^2 - F_c^2)^2]/(n-p)\}^{1/2}$. $R_1 = \Sigma||F_o| - |F_c||/\Sigma|F_o|$. $wR_2 = \{\Sigma[w(F_o^2 - F_c^2)^2]/\Sigma[w(F_o^2)^2]\}^{1/2}$. $w = 1/[\sigma^2(F_o^2) + (aP)^2 + bP]$ where a is 0.0339, b is 2.0112, and P is $[2F_c^2 + \text{Max}(F_o^2,0)]/3$.

DISCUSSION OF THE STRUCTURE

General description of the structure

The structure of whelanite (Figs. 5a and 5b) contains two different types of polyhedral layers parallel to {001}, which alternate along [001] and are linked to one another by sharing corners with silicate groups in the layer region. One polyhedral layer, consisting of edge-sharing CaO_7 polyhedra, is identical to that in the structures of the tobermorites (tobermorite 9Å, tobermorite 11Å, tobermorite 14Å, and clinotobermorite). The other layer is brucite-like, with ribbons of edge-sharing Jahn-Teller distorted $Cu^{2+}O_6$ octahedra along [010] alternating with ribbons of edge-sharing CaO_6 octahedra (Fig. 6). The edge-sharing octahedral layer with alternating ribbons of $Cu^{2+}O_6$ and CaO_6 octahedra has not previously been reported in any mineral.

The linkage of the silicate groups is not immediately obvious because of the disorder manifest in this portion of the structure. An examination of the order-disorder (OD) character of the structure (see below) allowed us to rationalize the silicate region as consisting of two overlapping half-occupied wollastonite-like silicate chains running parallel [010] (Fig. 7). The chemical and Raman investigations indicate the presence of CO_3 and H_2O groups and these must presumably also be hosted in the interlayer region. We discuss their possible dispositions below.

The OD character of whelanite

OD theory was developed by Dornberger-Schiff (1956, 1964, 1966) to deal with order-disorder aspects and polytypic features

[1] Deposit item AM-12-081, CIF and structure factors. Deposit items are available two ways: For a paper copy contact the Business Office of the Mineralogical Society of America (see inside front cover of recent issue) for price information. For an electronic copy visit the MSA web site at http://www.minsocam.org, go to the *American Mineralogist* Contents, find the table of contents for the specific volume/issue wanted, and then click on the deposit link there.

in structures characterized by ambiguities in the stacking of adjacent structural layers. A recent account of OD theory may be found in Ferraris et al. (2008).

The average structure of whelanite, described above, was derived from the refinement using the "family reflections", i.e., those reflections related to the subcell (A = 5.655, B = 3.6835, C = 27.137 Å, and space group $Pn2n$).

The part of the real structure that may be derived from these data (subcell reflections) is formed by two modules corresponding to the two kinds of polyhedral layers: the tobermorite-like CaO_7 layer module and the $Cu^{2+}O_6$–CaO_6 octahedra layer module. These two modules in fact have repeat periods of A = 5.655 and B = 3.6835 Å in the (**a**,**b**) plane.

The structure of whelanite may be completed with the insertion of wollastonite chains between the above modules. The way in which the wollastonite chains are grasped to the tobermorite-like module is described in Merlino et al. (2000).

Adjacent wollastonite chains on the same side of the tobermorite-like module are shifted by **b**/2, whereas chains on the opposite sides of the module are shifted by ±**b**/4. In Figure 5c, the fractional height of the wollastonite chains is reported, with reference to the true periodicity along **b**, namely 7.367 Å.

The single OD layer (indicated in Fig. 5c by the square bracket) has layer group symmetry $C12(1)$, with translation vectors **a** and **b** (a = 11.310, b = 7.367 Å), and the third vector $\mathbf{c_0}$ (c_0 = 13.569 Å).

Among the possible OD groupoid families corresponding to the layer group $C12(1)$ (Dornberger-Schiff and Fichtner 1972;

TABLE 4. Fractional coordinates, occupancies and atom displacement parameters (Å²) for whelanite

	x	y	z	Occ.	U_{eq}	U_{11}	U_{22}	U_{33}	U_{23}	U_{13}	U_{12}
Cu	0.0000	0.0000	0.0000	0.920(7)	0.0161(6)	0.0084(8)	0.0238(9)	0.0160(9)	0.000	0.0012(6)	0.000
Ca1	0.5000	0.504(3)	0.0000	1	0.0166(6)	0.0145(11)	0.0161(13)	0.0192(13)	0.000	–0.0009(10)	0.000
Ca2	0.6498(2)	0.999(2)	0.78612(5)	1	0.0121(5)	0.0111(8)	0.0085(9)	0.0165(9)	–0.007(3)	–0.0005(7)	–0.003(3)
Si1a	0.650(2)	0.097(4)	0.6730(5)	0.50	0.0100(8)						
Si1b	0.652(2)	0.932(4)	0.6733(4)	0.50	0.0100(8)						
Si2	0.8015(7)	0.514(4)	0.59994(14)	0.50	0.0128(11)						
O1	0.3767(8)	0.501(5)	0.79316(17)	1	0.0124(11)	0.012(2)	0.014(3)	0.011(3)	0.006(9)	0.002(2)	0.005(9)
O2	0.9147(8)	0.498(5)	0.79607(18)	1	0.0165(12)	0.011(2)	0.015(3)	0.024(3)	0.005(12)	0.002(2)	–0.002(9)
O3	0.6983(8)	0.009(5)	0.03921(17)	1	0.0178(13)	0.015(3)	0.021(3)	0.018(3)	0.004(10)	0.002(2)	0.001(8)
O4	0.3914(13)	0.007(6)	0.1224(2)	1	0.051(2)	0.076(5)	0.054(5)	0.024(4)	–0.017(12)	–0.007(3)	0.002(14)
O5	0.1627(13)	0.668(3)	0.0440(3)	1	0.039(2)	0.020(4)	0.058(5)	0.039(5)	0.017(4)	–0.002(4)	0.004(4)
O6a	0.664(4)	0.843(7)	0.6234(8)	0.50	0.015(2)						
O6b	0.668(4)	0.132(6)	0.6184(8)	0.50	0.015(2)						
O7	0.6448(15)	0.511(5)	0.6515(3)	0.50	0.013(2)						

TABLE 5. Selected bond distances (Å) and angles (°) for whelanite

Cu-O5 (×2)	1.941(9)	Si1a-O2	1.614(14)	Si1b-O1	1.583(14)	Si2-O6a	1.57(3)
Cu-O3 (×2)	2.011(5)	Si1a-O1	1.616(14)	Si1b-O2	1.598(13)	Si2-O3	1.648(6)
Cu-O5 (×2)	2.886(10)	Si1a-O7	1.634(15)	Si1b-O7	1.660(15)	Si2-O6b	1.68(2)
<Cu-O>	2.279	Si1a-O6a	1.64(3)	Si1b-O6b	1.66(3)	Si2-O4	1.840(8)
		<Si1a-O>	1.63	<Si1b-O>	1.63	<Si2-O>	1.68
Ca1-O5 (×2)	2.331(8)						
Ca1-O3 (×2)	2.390(15)	O2-Si1a-O1	108.0(8)	O1-Si1b-O2	110.5(7)	O6a-Si2-O3	114.4(11)
Ca1-O3 (×2)	2.419(15)	O2-Si1a-O7	112.4(11)	O1-Si1b-O7	112.1(10)	O6a-Si2-O6b	107.7(5)
<Ca1-O>	2.380	O2-Si1a-O6a	109.8(12)	O1-Si1b-O6b	113.6(11)	O6a-Si2-O4	110.0(11)
		O1-Si1a-O7	114.8(10)	O2-Si1b-O7	107.9(11)	O3-Si2-O6b	106.8(11)
Ca2-O2	2.385(16)	O1-Si1a-O6a	107.7(12)	O2-Si1b-O6b	116.2(11)	O3-Si2-O4	109.3(3)
Ca2-O2	2.393(16)	O7-Si1a-O6a	103.8(12)	O7-Si1b-O6b	95.5(11)	O6b-Si2-O4	108.5(11)
Ca2-O1	2.406(13)	<O-Si1a-O>	109.4	<O-Si1a-O>	109.3	<O-Si1a-O>	109.5
Ca2-O1	2.417(14)						
Ca2-O4	2.495(8)						
Ca2-O1	2.505(5)						
Ca2-O2	2.597(5)						
<Ca2-O>	2.457						

TABLE 6. Bond valence sums for whelanite (values are expressed in valence units)

	Cu	Ca1	Ca2	Si1a	Si1b	Si2	Σ	Σ*
O1			0.31, 0.30 0.24	1.03 ×½→	1.12 ×½→		1.93	
O2			0.33, 0.32 0.18	1.02 ×½→	1.07 ×½→		1.88	
O3	0.41 × 2↓	0.32 × 2↓ 0.30 × 2↓				0.94	1.97	1.03
O4			0.24			0.56	0.80	0.24
O5	0.49 × 2↓ 0.04 × 2↓	0.38 × 2↓					0.91	
O6a				0.96		1.16	2.12	
O6b					0.91	0.86	1.77	
O7				0.97	0.91		1.88	
Σ	1.88	2.00	1.92	3.98	4.01	3.52		

Notes: Multiplicity is indicated by ×→↓. Cu^{2+}-O and Ca^{2+}-O bond strengths from Brown and Altermatt (1985). Si^{4+}-O bond strength from Brese and O'Keeffe (1991). The last column headed by Σ* indicates the bond-valence sums for O3 and O4 when they do not participate in bonding to Si2.

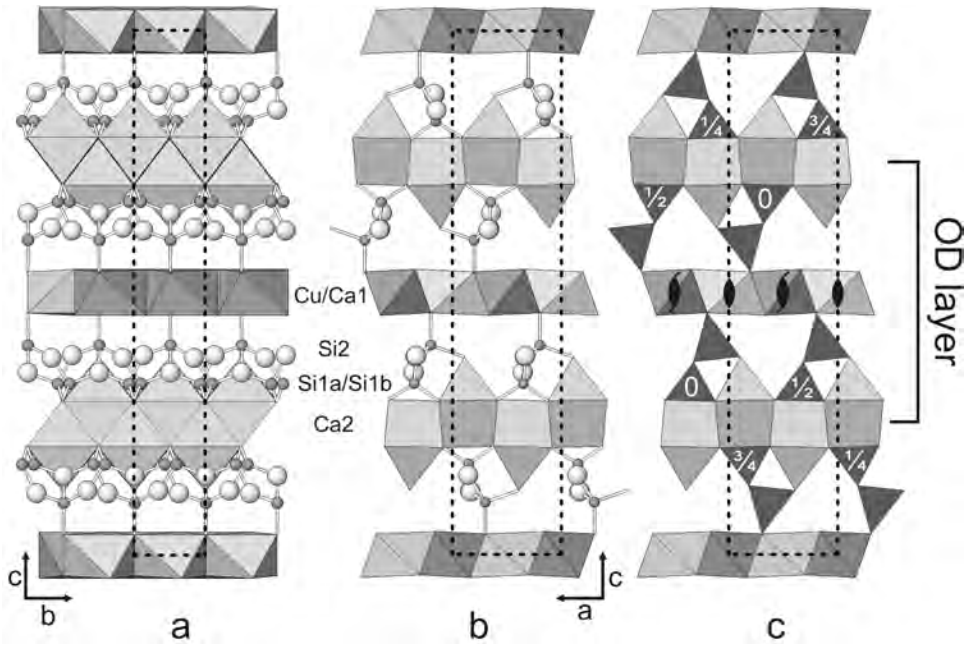

FIGURE 5. The crystal structure of whelanite (**a**) down [100], (**b**) down [010], and (**c**) down [010] showing OD features.

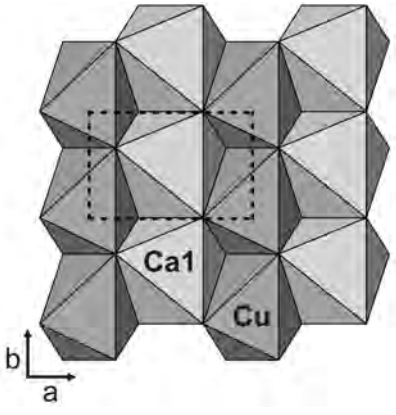

FIGURE 6. The brucite-like edge-sharing layer of octahedra in the structure of whelanite viewed down [001].

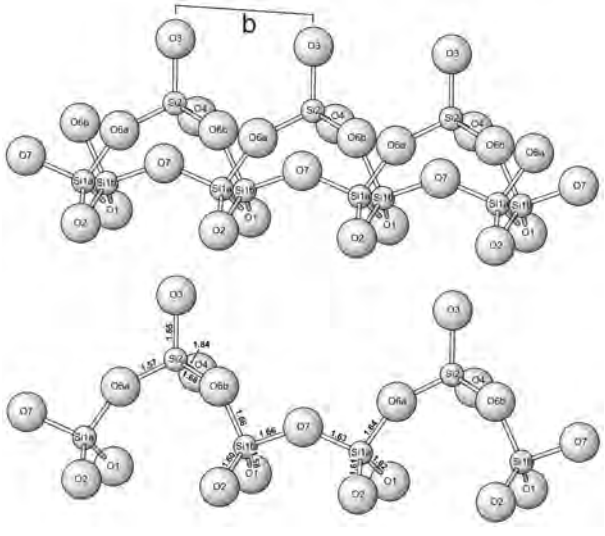

FIGURE 7. The overlapping, half-occupied, wollastonite-like silicate chains in whelanite (**top**) and only one of the chains (**bottom**); clinographic projection viewed approximately down [100]. The unit cell repeat along the **b**-axis is shown.

Ferraris et al. 2008), we found

$$\begin{matrix} C & 1 & 2 & (1) \\ \{ & n_{1/2,2} & 1\,(n_{1/2,1/2}) & \} \end{matrix} \qquad (1)$$

whose partial operations are compatible with the symmetry (*Pn*2*n*) of the family structure, which has the following basic vectors: **A** = **a**/2, **B** = **b**/2, and **C** = 2**c**$_0$.

The symbol (1) indicates that layers with symmetry *C* 1 2 1 may follow each other in the **c** direction, related by the operators $n_{1/2,2}$ (or $n_{-1/2,2}$) normal to **a** [and $n_{1/2,1/2}$ (or $n_{1/2,-1/2}$) normal to **c**].

There are two maximum degree of order (MDO) polytypes in this family: MDO1, corresponding to the sequence of OD layers in which the operators $n_{1/2,1/2}$ and $n_{1/2,-1/2}$ normal to **c** regularly alternate, and MDO2, corresponding to the sequence of layers in which the operator $n_{1/2,1/2}$ is constantly applied (the constant application of the operator $n_{1/2,-1/2}$ gives rise to the structure MDO2′, in twin relation with MDO2).

The space group symmetry and the unit-cell parameters of the two MDO polytypes may be reliably derived as follows.

MDO1. The σ-operator $n_{1/2,2}$ normal to **a** is continuing in the succeeding layers, becoming a total glide [*d* – –] in a structure with **c** = 4**c**$_0$; the *C*-centering operator **a**/2 + **b**/2 is valid for all the layers and the σ-operators $n_{1/2,1/2}$ and $n_{1/2,-1/2}$ become total [– – *d*]

glides; the twofold axes parallel to **b** of the single layers (λ operators) are valid for the whole structure. Therefore, the MDO1 polytype is orthorhombic, with space group symmetry *Fd2d*, and unit-cell parameters $a = 11.310$, $b = 7.367$, $c = 54.274$ Å.

MDO2. The application of two successive operators $n_{1/2,1/2}$ (normal to **c**) corresponds to a translation $2\mathbf{c_0} + (\mathbf{a}+\mathbf{b})/2$. As all the layers are *C*-centered, the third layer is actually translated by $\mathbf{c} = 2\mathbf{c_0}$ relatively to the first one. Apart from the $(\mathbf{a}+\mathbf{b})/2$ translation, none of the λ- or σ-operators is valid for the whole structure. Therefore the MDO2 polytype is triclinic, with space-group symmetry *C*1 and unit-cell parameters $a = 11.310$, $b = 7.367$, $c = 27.137$ Å, $\alpha = 90°$, $\beta = 90°$, and $\gamma = 90°$. This cell could be transformed into a reduced primitive cell, but the *C*-centered one is preferred to make easier comparison with the MDO1 polytype and with the cell of the "family structure."

The silicate chains

Figure 7 shows all of the located sites associated with the silicate groups, with the likely Si-O bonds shown. The complex array of sites actually consists of two overlapping half-occupied wollastonite-like silicate chains. A similar situation has been described by Hoffmann and Armbruster (1997) in their refinement of the substructure of clinotobermorite. Other than the very long Si2-O4 bond, mentioned above, and the rather small O7-Si1b-O6b angle, 95.5°, the silicate groups have reasonable bond lengths and geometries (see Table 5). The chain is linked via the sequence -Si2-O6b-Si1b-O7-Si1a-O6a-Si2-. All of the O atoms that form the Si-O-Si links (O6a, O6b, and O7) are half-occupied, consistent with the fact that each of the overlapping chains is present only half of the time. Note that O6a is occupied when the adjacent Si1a site is occupied and the same is true for the O6b-Si1b pair. The O1, O2, O3, and O4 atoms form peripheral silicate vertices and all are fully occupied. Atoms O1 and O2 participate in both of the overlapping silicate chains and, therefore, are always silicate O atoms. On the other hand, O3 and O4 are only silicate O atoms half of the time. Both O3 and O4 are candidates for participating in a CO_3 group, but if they do not, O3 must be an OH and O4 must be an H_2O, based on bond-valence considerations (Table 6).

The O4 has significantly higher thermal displacement parameters (especially U_{11} and U_{22}) than any of the other O atoms. This may help to explain the very long Si2-O4 bond noted above. When the O4 is an H_2O and does not participate in the Si2 silicate group, it moves closer to Ca2; when it participates in the Si2 silicate group, it moves closer to Si2 and further from Ca2. As it stands, the bond-valence sum for O4 when it is bonded to Si2 is 0.80, but even with a normal Si2-O4 bond length, O4 would be significantly undersaturated in bond strength, suggesting that it has at least some OH (silanol) character when participating as part of the silicate chain. Nyfeler and Armbruster (1998) note that the Si-OH bond-length tends to be only modestly longer than the other Si-O bonds for silicate groups with two bridging O atoms (such as in whelanite), so this certainly does not explain the very long 1.84 Å bond length, but it is consistent with Si2-O4 being longer that the other Si-O bonds. For derivation of the ideal formula (see below), we assume that O4 has partial (½) OH character when participating in the silicate chain, i.e., ¼ OH character overall.

Where is the carbonate?

In spite of concerted efforts to locate and/or model the CO_3 group in the whelanite structure, no conclusive evidence for its placement was found. Existing O sites that could participate in a CO_3 group based upon bond-valence sums and geometric constraints are O3, O4, and O5. As noted above, O3 and O4 take part in the Si2 silicate group, but only half of the time. The other half of the time O3 must be either an OH group or a corner of the CO_3 group. If the latter is the case, and it has a normal bond length to C, it would be significantly oversaturated in bond strength (1.03 + 1.33 = 2.36 v.u.). When O4 is not bonded to Si2, it is either an H_2O group or a corner of the CO_3 group, but if the latter is the case, it would remain significantly undersaturated in bond strength (0.24 + 1.33 = 1.57 v.u.), unless it received multiple hydrogen bonds. The final possible participant in the CO_3 group is O5. From a bond-valence perspective, this presents the most attractive choice as it would be closer to bond-valence balanced (0.91 + 1.33 = 2.24 v.u.) and a somewhat longer than average C-O5 bond would improve matters. Furthermore, there appears to be plenty of space in the interlayer region adjacent to O5 to accommodate a CO_3 group. Examining residual electron density in the vicinities of the O3, O4, and O5 sites, indicates that significant residuals in the interlayer region are only present near the O5 site, including a 0.36 peak at [0.017, 0.500, 0.069] 1.24 Å from O5. Our attempt to refine this residual as a partially occupied C site were only marginally successful, in that no other sites could be located to successfully complete the CO_3 group. In the end, we are left to conclude that the CO_3 group is too disordered to be located using the existing structure data, but that its location in the interlayer region, bonded to O5, appears to be the most likely.

The ideal formula of whelanite

The original formula proposed for whelanite, $Cu_2Ca_5Si_6O_{17}(CO_3)(OH)_2{\cdot}4H_2O$, was based only on the chemical analyses. Although our structure determination failed to locate the CO_3 group, it does provide sufficient new information to better define the chemical formula. The total number of O sites provides 26 O apfu, and this is the basis we have used for calculating the empirical formula.

Using full Cu occupancy and ignoring C and H, the ideal formula thereby obtained is $[Cu_2Ca_6Si_6O_{26}]^{12-}$. Still neglecting C, bond-valence considerations indicate O5 to be OH, O3 to be ½ O and ½ OH, and O4 to be ¼ O, ¼ OH, and ½ H_2O (see above), yielding $[Cu_2Ca_6Si_6O_{17}(OH)_7(H_2O)_2]^{1-}$. Now the assumptions become more tenuous because of our failure to model the CO_3 group. Based upon the relatively low-electron density residuals, we prefer to assume that our structure refinement has accounted for all of the O atoms (26) and that any "additional" O atoms needed for the CO_3 group are balanced by small deficiencies in some of the located O sites. Furthermore, based upon the chemical analyses, we believe it best to use one CO_3 group pfu for the ideal formula. As a final assumption, we think it is most reasonable to replace a portion of the OH in the formula (corresponding principally with the O5 site) with CO_3. The resulting ideal formula for whelanite is $Cu_2Ca_6[Si_6O_{17}(OH)](CO_3)(OH)_3(H_2O)_2$, which is a reasonably good fit for the analyzed composition.

Related structures

As we have already noted, the calcium polyhedral layer in whelanite is very similar to that occurring in the minerals of the tobermorite group. The 9, 11, and 14 Å tobermorite structures (Merlino et al. 2000, 2001; Bonaccorsi et al. 2005) contain successively larger spacings between adjacent CaO_7 polyhedra layers. In tobermorite 11Å the wollastonite chains are connected to give double chains, whereas in tobermorite 9Å decondensation occurs and adjacent layers of Ca polyhedra approach each other. The tobermorite 14Å structure is the most similar to that of whelanite: both structures are characterized by the presence of single wollastonite chains of Si tetrahedra, which are connected on one side, by edge sharing, to the layer of CaO_7 polyhedra, and on the other side, by corner sharing, to octahedra in the interlayer region; however, whereas the interlayer region of tobermorite 14Å hosts columns of CaO_6 octahedra (Bonaccorsi et al. 2005), that of whelanite has a continuous brucite-like layer built up by columns of CaO_6 and CuO_6 octahedra.

The structures of dovyrenite (Kadiyski et al. 2008), roumaite (Biagioni et al. 2010), and rinkite (Cámara et al. 2011) all contain tobermorite-like layers of edge-sharing CaO_7 polyhedra, which alternate with modified brucite-like layers of edge-sharing octahedra, and have silicate linkages in between. However, these structures differ from that of whelanite in two important respects: (1) all three contain Si_2O_7 (disilicate) groups, rather than wollastonite-like chains, and (2) the tobermorite-like and brucite-like layers link directly to each other by corner-sharing.

The fukalite structure (Merlino et al. 2009) also exhibits some similarity to that of whelanite. Here, tobermorite-like layers alternate with tilleyite-like corrugated layers of edge-sharing six- and seven-coordinated Ca polyhedra. Between the layers are silicate chains, but not with a wollastonite-like configuration. Another intriguing similarity is the presence of a CO_3 group, which in fukalite shares an edge with the CaO_7 polyhedron of the tobermorite-like layer. This suggests the possibility that the unlocated CO_3 group in whelanite may assume a similar position; however, in whelanite the corresponding CaO_7 polyhedral edge is O1-O2, which is clearly part of the silicate chain.

Finally, it is worth noting that all of the aforementioned structures related to that of whelanite exhibit OD character.

Acknowledgments

Reviewers Fernando Cámara and Daniel Atencio and Associate Editor Fernando Colombo provided helpful comments on the manuscript. John Magnasco is thanked for information on the occurrences of whelanite, for his ongoing encouragement through the many often-frustrating years of this study and for providing specimens of whelanite from the Christmas mine and the Sunrise prospect. Sharon Cisneros is thanked for providing a specimen of whelanite from the Christmas mine. The late Fred Devito provided some specimens of the whelanite-like mineral (mineral Y) from Crestmore and later Thomas Loomis provided others from the Devito collection. Elena Sokolova is thanked for comments on some of the structural relationships. Frank Hawthorne, Peter Burns, Uwe Kolitsch, and Robert Downs are thanked for providing information regarding previous attempts to solve the whelanite structure. This study was funded by the John Jago Trelawney Endowment to the Mineral Sciences Department of the Natural History Museum of Los Angeles County.

References cited

Biagioni, C., Bonaccorsi, E., Merlino, S., Parodi, G.C., Perchiazzi, N., Chevrier, V., and Bersani, D. (2010) Roumaite, $(Ca,Na,\square)_3(Ca,REE,Na)_4(Nb,Ti)[Si_2O_7]_2(OH)F_3$, from Rouma Island, Los Archipelago, Guinea: a new mineral species related to dovyrenite. Canadian Mineralogist, 48, 17–28.

Bonaccorsi, E., Merlino, S., and Kampf, A.R. (2005) The crystal structure of tobermorite 14Å (plombierite), a C-S-H phase. Journal of the American Ceramic Society, 88, 505–512.

Brese, N.E. and O'Keeffe, M. (1991) Bond-valence parameters for solids. Acta Crystallographica B, 47, 192–197.

Brown, I.D. and Altermatt, D. (1985) Bond-valence parameters from a systematic analysis of the inorganic crystal structure database. Acta Crystallographica B, 41, 244–247.

Cámara, F., Sokolova, E., and Hawthorne, F.C. (2011) From structure topology to chemical composition. XII. Titanium silicates: the crystal chemistry of rinkite, Na_2Ca_4*REE*$Ti(Si_2O_7)_2OF_3$. Mineralogical Magazine, 75, 2755–2774.

Dornberger-Schiff, K. (1956) On the order-disorder structures (OD-structures). Acta Crystallographica, 9, 593–601.

——— (1964) Grundzüge einer Theorie von OD-Strukturen aus Schichten. Abhandlungen der Deutschen Akademie der Wissenschaften zu Berlin, Klasse für Chemie, Geologie und Biologie, 3, 1–107.

——— (1966) Lehrgang über OD-Strukturen. Akademie-Verlag, Berlin, 135 p.

Dornberger-Schiff, K. and Fichtner, K. (1972) On the symmetry of OD-structures consisting of equivalent layers. Kristall und Technik, 7, 1035–1056.

Ferraris, G., Makovicky, E., and Merlino, S. (2008) Crystallography of modular materials. IUCr Monographs on Crystallography, 15, Oxford University Press, New York, 372 p.

Flack, H.D. and Bernardinelli, G. (1999) Absolute structure and absolute configuration. Acta Crystallographica A, 55, 908–915.

Frost, R.L. and Xi, Y. (2012) Whelanite $Ca_5Cu_2(OH)_2CO_3Si_6O_{17}{\cdot}4H_2O$ – A vibrational spectroscopic study. Spectrochimica Acta Part A: Molecular and Biomolecular Spectroscopy, 91, 319–323.

Gunter, M.E., Bandli, B.R., Bloss, F.D., Evans, S.H., Su, S.C., and Weaver, R. (2004) Results from a McCrone spindle stage short course, a new version of EXCALIBR, and how to build a spindle stage. The Microscope, 52, 23–39.

Higashi, T. (2001) ABSCOR. Rigaku Corporation, Tokyo, Japan.

Hindman, J.R. (1976) Stringhamite, a new hydrous copper calcium silicate from Utah. American Mineralogist, 61, 189–192.

Hintze, L.F. and Whelan, J.A. (1973) Geology of the Milford area. Utah Geological Association, Publication 3.

Hoffmann, C. and Armbruster, T. (1997) Clinotobermorite $Ca_5[Si_3O_8(OH)_2{\cdot}4H_2O$–$Ca_5[Si_6O_{17}]{\cdot}5H_2O$, a natural C-S-H(I) cement mineral: determination of the substructure. Zeitschrift für Kristallographie, 212, 864–873.

Kadiyski, M., Armbruster, T., Galuskin, E.V., Pertsev, N.N., Zadov, A.E., Galuskina, I.O., Wrzalik, R., Dzierzanowski, P., and Kislov, E.V. (2008) The modular structure of dovyrenite, $Ca_6Zr[Si_2O_7]_2(OH)_4$: Alternate stacking of tobermorite and rosenbuschite-like units. American Mineralogist, 93, 456–462.

Mandarino, J.A. (1981) The Gladstone-Dale relationship: Part IV. The compatibility concept and its application. Canadian Mineralogist, 19, 441–450.

Merlino, S., Bonaccorsi, E., and Armbruster, T. (2000) The real structure of clinotobermorite and tobermorite 9Å: OD character, polytypes, and structural relationships. European Journal of Mineralogy, 12, 411–429.

——— (2001) The real structure of tobermorite 11Å: normal and anomalous forms, OD character and polytypic modifications. European Journal of Mineralogy, 13, 577–590.

Merlino, S., Bonaccorsi, E., Grabezhev, A.I., Zadov, A.E., Pertsev, N.N., and Chukanov, N.V. (2009) Fukalite: An example of an OD structure with two-dimensional disorder. American Mineralogist, 94, 323–333.

Morrison, S.M., Downs, R.T., and Yang, H. (2012) Redetermination of the kovdorskite, $Mg_2PO_4(OH){\cdot}3H_2O$. Acta Crystallographica Section E Structural Reports Online, 68, 12–13.

Murdoch, J. (1961) Crestmore, past and present. American Mineralogist, 46, 245–257.

Nyfeler, D. and Armbruster, T. (1998) Silanol groups in minerals and inorganic compounds. American Mineralogist, 83, 119–125.

Sheldrick, G.M. (2008) A short history of SHELX. Acta Crystallographica A, 64, 112–122.

Wray, W.B. (2006) Mines and geology of the Rocky and Beaver Lake districts, Beaver County, Utah. Utah Geological Association Publication 32, Mining Districts of Utah, 183–285.

Manuscript received March 28, 2012
Manuscript accepted July 9, 2012
Manuscript handled by Fernando Colombo

h	k	l	10Fo	10Fc	10s	h	k	l	10Fo	10Fc	10s	h	k	l	10Fo	10Fc	10s	h	k	l	10Fo	10Fc	10s	h	k	l	10Fo	10Fc	10s
3	-3	0	591	558	20	4	-2	3	364	349	10	5	1	5	67	61	20	3	-1	8	366	362	7	0	-3	11	258	234	12
2	-2	0	236	231	6	5	-2	3	0	46	1	1	2	5	62	67	17	4	-1	8	104	135	21	1	-3	11	124	127	28
4	-2	0	98	117	21	0	-1	3	365	376	9	2	2	5	123	140	18	5	-1	8	326	345	11	2	-3	11	104	127	29
1	-1	0	269	261	8	1	-1	3	682	689	13	3	2	5	289	276	6	0	0	8	350	331	11	3	-3	11	134	127	54
3	-1	0	1554	1531	30	2	-1	3	145	142	5	4	2	5	37	56	36	1	0	8	581	564	7	1	-2	11	370	372	18
5	-1	0	135	187	30	3	-1	3	85	94	12	5	2	5	100	123	13	2	0	8	698	713	6	2	-2	11	87	91	22
2	0	0	46	23	46	4	-1	3	44	80	44	0	3	5	25	44	24	3	0	8	242	247	11	3	-2	11	260	234	13
4	0	0	401	402	8	5	-1	3	348	322	12	1	3	5	124	145	11	4	0	8	698	702	7	4	-2	11	0	46	1
6	0	0	805	805	16	1	0	3	132	114	7	2	3	5	0	21	1	5	0	8	340	335	8	0	-1	11	429	440	6
1	1	0	258	256	5	2	0	3	211	216	9	3	3	5	70	77	37	1	1	8	763	760	5	1	-1	11	276	260	4
3	1	0	1584	1533	25	3	0	3	199	184	5	1	-3	6	461	432	17	2	1	8	741	735	8	2	-1	11	224	234	5
5	1	0	187	185	12	4	0	3	471	464	7	2	-3	6	264	267	11	3	1	8	368	360	6	3	-1	11	178	175	10
0	2	0	2109	1983	49	5	0	3	83	61	19	3	-3	6	189	177	15	4	1	8	141	133	11	4	-1	11	401	386	11
2	2	0	235	228	31	6	0	3	58	52	45	0	-2	6	608	592	9	5	1	8	360	345	18	5	-1	11	227	247	11
4	2	0	105	114	19	0	1	3	370	374	8	1	-2	6	113	142	15	0	2	8	251	251	7	1	0	11	451	447	6
1	3	0	151	151	8	1	1	3	690	690	8	2	-2	6	508	529	13	1	2	8	468	463	5	2	0	11	101	79	14
3	3	0	558	559	29	2	1	3	141	144	7	3	-2	6	71	100	35	2	2	8	486	494	7	3	0	11	166	169	7
2	-3	1	158	154	15	3	1	3	94	94	7	4	-2	6	261	255	9	3	2	8	140	179	14	4	0	11	53	72	27
3	-3	1	83	123	26	4	1	3	62	83	23	5	-2	6	137	137	43	4	2	8	525	507	9	5	0	11	0	24	1
1	-2	1	52	78	37	5	1	3	320	323	8	1	-1	6	690	683	4	1	3	8	383	398	6	0	1	11	436	441	8
2	-2	1	325	311	5	1	2	3	164	157	5	2	-1	6	672	671	7	2	3	8	365	388	12	1	1	11	277	260	7
3	-2	1	372	360	10	2	2	3	205	205	10	3	-1	6	542	527	8	3	3	8	222	233	12	2	1	11	221	233	9
4	-2	1	225	239	9	3	2	3	0	27	1	4	-1	6	150	153	15	0	-3	9	338	330	8	3	1	11	149	175	10
5	-2	1	107	75	22	4	2	3	331	349	13	5	-1	6	448	434	11	1	-3	9	139	141	28	4	1	11	386	386	11
0	-1	1	439	457	7	5	2	3	24	46	23	0	0	6	1050	1066	15	2	-3	9	56	79	56	5	1	11	201	247	19
1	-1	1	715	699	6	0	3	3	91	80	17	1	0	6	546	576	6	3	-3	9	0	25	1	1	2	11	367	371	7
2	-1	1	63	75	16	1	3	3	390	391	5	2	0	6	724	726	6	1	-2	9	290	302	8	2	2	11	85	90	9
3	-1	1	274	272	7	2	3	3	114	148	12	3	0	6	127	128	14	2	-2	9	67	58	33	3	2	11	241	234	14
4	-1	1	235	229	12	3	3	3	0	36	1	4	0	6	258	260	9	3	-2	9	611	591	11	4	2	11	0	45	1
5	-1	1	576	542	13	1	-3	4	266	249	20	5	0	6	304	291	11	4	-2	9	112	147	11	0	3	11	240	234	9
1	0	1	225	203	3	2	-3	4	525	506	11	1	1	6	694	684	6	0	-1	9	757	763	9	1	3	11	120	127	22
2	0	1	663	665	5	3	-3	4	499	478	16	2	1	6	676	672	7	1	-1	9	338	347	5	2	3	11	129	126	10
3	0	1	101	86	9	0	-2	4	740	711	12	3	1	6	553	527	5	2	-1	9	89	106	11	3	3	11	91	127	19
4	0	1	420	421	6	1	-2	4	348	358	8	4	1	6	142	154	8	3	-1	9	20	23	20	1	-3	12	495	481	36
5	0	1	0	16	1	2	-2	4	479	482	13	5	1	6	427	435	10	4	-1	9	194	204	10	2	-3	12	167	155	20
6	0	1	246	265	15	3	-2	4	25	47	25	0	2	6	603	591	12	5	-1	9	290	286	10	3	-3	12	171	130	32
0	1	1	440	453	6	4	-2	4	238	230	11	1	2	6	118	144	10	1	0	9	556	550	6	0	-2	12	44	79	43
1	1	1	711	698	5	5	-2	4	50	74	50	2	2	6	522	530	7	2	0	9	88	66	14	1	-2	12	258	239	30
2	1	1	83	80	9	1	-1	4	719	739	11	3	2	6	88	100	20	3	0	9	939	908	9	2	-2	12	408	426	11
3	1	1	272	272	7	2	-1	4	606	606	6	4	2	6	262	255	10	4	0	9	229	229	7	3	-2	12	44	64	44
4	1	1	239	230	10	3	-1	4	586	587	8	5	2	6	157	138	17	5	0	9	70	91	29	4	-2	12	560	546	13
5	1	1	547	542	12	4	-1	4	98	111	19	1	3	6	422	433	6	0	1	9	767	766	8	1	-1	12	953	941	8
1	2	1	65	82	11	5	-1	4	414	410	13	2	3	6	271	267	14	1	1	9	350	348	4	2	-1	12	397	400	6
2	2	1	312	311	4	0	0	4	791	789	11	3	3	6	168	175	13	2	1	9	98	103	16	3	-1	12	195	202	6
3	2	1	364	358	6	1	0	4	118	118	9	1	-3	7	103	93	24	3	1	9	43	23	43	4	-1	12	304	319	10
4	2	1	233	239	7	2	0	4	761	766	6	2	-3	7	176	204	19	4	1	9	199	203	8	5	-1	12	331	348	10
5	2	1	75	75	22	3	0	4	108	99	8	3	-3	7	40	51	39	5	1	9	322	286	11	1	0	12	458	455	8
0	3	1	493	457	8	4	0	4	421	410	5	1	-2	7	377	380	19	1	2	9	292	300	6	2	0	12	715	723	7
1	3	1	138	162	10	5	0	4	129	139	13	2	-2	7	79	103	25	2	2	9	51	59	26	3	0	12	78	69	14
2	3	1	131	153	9	6	0	4	323	301	18	3	-2	7	398	403	10	3	2	9	606	592	9	4	0	12	740	731	9
3	3	1	78	123	17	1	1	4	742	739	8	4	-2	7	196	184	9	4	2	9	118	147	19	5	0	12	229	235	21
2	-3	2	256	257	18	2	1	4	603	605	5	5	-2	7	86	119	36	0	3	9	334	329	10	1	1	12	956	942	9
3	-3	2	120	154	16	3	1	4	593	589	5	0	-1	7	62	70	19	1	3	9	125	141	15	2	1	12	404	400	7
1	-2	2	152	144	11	4	1	4	91	110	14	1	-1	7	124	137	9	2	3	9	56	79	37	3	1	12	188	200	10
2	-2	2	474	496	5	5	1	4	410	410	9	2	-1	7	464	461	3	3	3	9	0	26	1	4	1	12	317	319	7
3	-2	2	185	168	11	0	2	4	730	711	8	3	-1	7	0	34	1	1	-3	10	143	144	19	5	1	12	347	348	10
4	-2	2	842	818	15	1	2	4	347	357	5	4	-1	7	207	202	8	2	-3	10	315	312	19	0	2	12	59	76	18
5	-2	2	51	38	50	2	2	4	488	482	8	5	-1	7	176	143	17	3	-3	10	538	495	16	1	2	12	241	240	4
1	-1	2	1010	1038	8	3	2	4	13	46	13	1	0	7	546	566	6	0	-2	10	1077	1025	17	2	2	12	414	426	9
3	-1	2	356	361	7	4	2	4	250	230	9	3	0	7	589	577	5	1	-2	10	355	360	11	3	2	12	117	64	18
4	-1	2	286	279	8	5	2	4	11	71	11	4	0	7	94	100	12	2	-2	10	366	389	19	4	2	12	536	546	10
5	-1	2	285	258	9	1	3	4	252	250	6	5	0	7	186	178	20	3	-2	10	174	190	14	1	3	12	486	481	7
2	0	2	539	578	5	2	3	4	499	506	9	0	1	7	56	72	28	4	-2	10	104	119	20	2	3	12	158	155	17
3	0	2	236	227	8	3	3	4	504	478	13	1	1	7	125	136	6	1	-1	10	344	362	6	3	3	12	136	130	23
4	0	2	1056	1057	11	1	-3	5	153	146	17	2	1	7	459	461	7	2	-1	10	686	686	6	0	-3	13	0	28	1
5	0	2	183	187	8	2	-3	5	0	19	1	3	1	7	22	34	22	3	-1	10	706	694	7	1	-3	13	365	331	61
6	0	2	183	180	12	3	-3	5	44	77	44	4	1	7	200	201	6	4	-1	10	167	157	10	2	-3	13	128	152	29
1	1	2	1004	1036	8	1	-2	5	67	65	22	5	1	7	137	143	10	5	-1	10	325	321	10	1	-2	13	189	191	5
2	1	2	240	212	6	2	-2	5	122	142	19	1	2	7	382	380	5	0	0	10	1321	1263	24	2	-2	13	175	166	14
3	1	2	367	363	5	3	-2	5	274	278	24	2	2	7	93	102	16	1	0	10	497	503	7	3	-2	13	25	86	25
4	1	2	274	279	6	4	-2	5	35	57	35	3	2	7	432	403	10	2	0	10	665	673	8	4	-2	13	225	228	26
5	1	2	238	256	8	5	-2	5	116	122	21	4	2	7	160	183	17	3	0	10	312	309	5	0	-1	13	289	289	11
0	2	2	179	176	21	0	-1	5	253	243	14	5	2	7	92	118	18	4	0	10	227	222	10	1	-1	13	364	365	5
1	2	2	139	144	6	1	-1	5	377	373	8	0	3	7	0	56	1	5	0	10	381	362	8	2	-1	13	161	180	9
2	2	2	475	494	6	2	-1	5	0	23	1	1	3	7	89	93	13	1	1	10	359	363	5	3	-1	13	0	17	1
3	2	2	165	168	9	3	-1	5	0	46	1	2	3	7	207	204	11	2	1	10	687	686	7	4	-1	13	92	105	15
4	2	2	822	818	12	4	-1	5	113	123	24	3	3	7	44	51	44	3	1	10	706	693	9	5	-1	13	165	171	14
5	2	2	27	37	26	5	-1	5	62	63	62	1	-3	8	410	399	17	4	1	10	143	157	10	1	0	13	118	125	12
1	3	2	515	540	6	1	0	5	147	138	9	2	-3	8	392	388	12	5	1	10	328	322	15	2	0	13	60	34	27
2	3	2	238	257	11	3	0	5	413	404	5	3	-3	8	238	232	17	0	2	10	1066	1025	14	3	0	13	148	142	7
3	3	2	136	155	16	4	0	5	276	282	7	0	-2	8	255	253	14	1	2	10	358	360	5	4	0	13	206	200	13
1	-3	3	385	391	13	5	0	5	112	128	14	1	-2	8	452	463	8	2	2	10	367	390	8	5	0	13	131	119	12
2	-3	3	128	149	28	0	1	5	256	238	5	2	-2	8	487	494	15	3	2	10	192	190	11	0	1	13	294	293	11
3	-3	3	0	36	1	1	1	5	382	372	6	3	-2	8	152	179	14	4	2	10	101	122	27	1	1	13	368	365	8
1	-2	3	141	156	12	2	1	5	38	29	25	4	-2	8	516	507	6	1	3	10	129	144	16	2	1	13	165	178	10
2	-2	3	197	203	10	3	1	5	49	45	22	1	-1	8	756	759	7	2	3	10	325	312	9	3	1	13	53	16	53
3	-2	3	47	30	47	4	1	5	99	124	12	2	-1	8	745	735	6	3	3	10	501	495	12	4	1	13	84	101	20

h	k	l	10Fo	10Fc	10s	h	k	l	10Fo	10Fc	10s	h	k	l	10Fo	10Fc	10s	h	k	l	10Fo	10Fc	10s	h	k	l	10Fo	10Fc	10s
5	1	13	130	170	23	5	0	15	206	224	26	4	0	17	92	66	19	3	2	19	405	390	12	2	2	22	197	217	28
1	2	13	194	191	7	0	1	15	0	53	1	0	1	17	262	257	11	0	3	19	280	248	28	1	-2	23	71	89	41
2	2	13	153	165	11	1	1	15	164	162	12	1	1	17	0	51	1	0	-2	20	430	394	9	2	-2	23	58	49	29
3	2	13	84	90	25	2	1	15	149	156	12	2	1	17	398	414	9	1	-2	20	269	270	9	0	-1	23	148	145	17
4	2	13	251	228	20	3	1	15	26	21	26	3	1	17	176	183	15	2	-2	20	269	289	21	1	-1	23	251	286	11
0	3	13	33	34	32	4	1	15	26	64	25	4	1	17	249	252	26	3	-2	20	0	40	1	2	-1	23	95	82	11
1	3	13	349	332	12	1	2	15	0	31	1	1	2	17	221	205	13	1	-1	20	597	602	8	3	-1	23	21	43	21
2	3	13	156	152	15	2	2	15	139	152	16	2	2	17	178	179	13	2	-1	20	358	375	13	1	0	23	5	34	4
1	-3	14	154	190	60	3	2	15	138	156	18	3	2	17	227	232	13	3	-1	20	111	104	17	2	0	23	121	162	31
2	-3	14	159	162	18	4	2	15	164	179	20	0	3	17	0	16	1	4	-1	20	85	128	39	3	0	23	121	99	28
0	-2	14	693	688	12	0	3	15	142	147	16	1	3	17	54	65	31	0	0	20	388	374	14	0	1	23	148	142	25
1	-2	14	160	166	5	1	3	15	247	236	15	1	-3	18	209	199	33	1	0	20	192	201	11	1	1	23	285	286	13
2	-2	14	476	473	11	2	3	15	68	112	22	0	-2	18	620	589	22	2	0	20	402	419	9	2	1	23	85	83	36
3	-2	14	68	68	67	1	-3	16	438	421	62	1	-2	18	65	52	25	3	0	20	41	37	41	3	1	23	81	43	34
4	-2	14	28	44	27	2	-3	16	327	301	13	2	-2	18	214	246	15	4	0	20	492	467	15	1	2	23	80	89	36
1	-1	14	600	618	6	0	-2	16	99	102	28	3	-2	18	108	130	37	1	1	20	615	602	10	2	2	23	0	49	1
2	-1	14	335	339	7	1	-2	16	341	336	6	1	-1	18	215	210	6	2	1	20	352	374	11	0	-2	24	599	592	17
3	-1	14	264	268	8	2	-2	16	600	589	17	2	-1	18	505	507	11	3	1	20	105	107	24	1	-2	24	19	39	18
4	-1	14	0	40	1	3	-2	16	0	31	1	3	-1	18	723	731	20	4	1	20	107	128	24	1	-1	24	69	90	25
5	-1	14	449	449	12	4	-2	16	477	468	14	4	-1	18	51	66	51	0	2	20	421	395	12	2	-1	24	44	59	44
0	0	14	592	579	12	1	-1	16	559	571	7	0	0	18	1016	978	18	1	2	20	273	269	10	3	-1	24	538	553	27
1	0	14	287	258	8	2	-1	16	672	667	9	1	0	18	191	185	11	2	2	20	276	288	22	0	0	24	1037	976	23
2	0	14	764	772	9	3	-1	16	145	153	13	2	0	18	258	260	10	3	2	20	87	40	27	1	0	24	20	37	20
3	0	14	114	133	13	4	-1	16	247	250	22	3	0	18	138	177	15	1	-2	21	202	212	11	2	0	24	180	243	24
4	0	14	178	186	16	0	0	16	122	79	21	4	0	18	94	93	16	2	-2	21	142	157	11	3	0	24	74	7	53
5	0	14	65	70	28	1	0	16	458	462	9	1	1	18	195	208	11	0	-1	21	84	116	31	1	1	24	88	89	23
1	1	14	596	619	9	2	0	16	718	727	10	2	1	18	510	508	11	1	-1	21	144	142	10	2	1	24	0	59	1
2	1	14	340	340	10	3	0	16	24	38	23	3	1	18	747	732	12	2	-1	21	0	16	1	3	1	24	569	553	21
3	1	14	262	263	9	4	0	16	502	515	12	4	1	18	61	67	39	3	-1	21	44	79	43	0	2	24	605	592	19
4	1	14	41	40	40	5	0	16	175	196	27	0	2	18	609	591	9	1	0	21	248	237	11	1	2	24	0	40	1
5	1	14	441	449	17	1	1	16	567	572	10	1	2	18	11	52	10	2	0	21	284	284	13	0	-1	25	105	121	23
0	2	14	715	684	9	2	1	16	679	667	11	2	2	18	243	245	18	3	0	21	12	20	12	1	-1	25	372	383	10
1	2	14	159	166	7	3	1	16	133	151	18	3	2	18	129	130	19	4	0	21	27	2	26	2	-1	25	111	123	21
2	2	14	471	474	11	4	1	16	212	250	26	1	3	18	197	198	15	0	1	21	92	115	29	1	0	25	131	154	17
3	2	14	66	68	37	0	2	16	110	99	19	0	-3	19	283	247	69	1	1	21	134	141	17	2	0	25	208	245	28
4	2	14	36	50	35	1	2	16	352	336	8	1	-2	19	102	108	21	2	1	21	0	15	1	3	0	25	0	61	1
1	3	14	181	192	9	2	2	16	595	590	10	2	-2	19	366	365	12	3	1	21	92	79	39	0	1	25	124	119	34
2	3	14	166	162	20	3	2	16	0	30	1	3	-2	19	414	391	16	1	2	21	204	213	13	1	1	25	402	383	11
0	-3	15	165	151	10	4	2	16	471	468	11	0	-1	19	420	410	8	2	2	21	168	157	26	2	1	25	90	124	26
1	-3	15	252	236	35	1	3	16	432	421	17	1	-1	19	627	628	7	0	-2	22	173	163	27	1	-1	26	483	500	9
2	-3	15	126	111	26	2	3	16	255	301	28	2	-1	19	114	133	15	1	-2	22	213	219	11	2	-1	26	30	58	29
1	-2	15	53	35	30	0	-3	17	0	13	1	3	-1	19	95	92	19	2	-2	22	184	218	19	0	0	26	23	91	22
2	-2	15	169	151	18	1	-3	17	105	65	63	4	-1	19	21	46	21	1	-1	22	354	356	7	1	0	26	0	2	1
3	-2	15	160	155	21	1	-2	17	211	205	12	1	0	19	103	102	19	2	-1	22	143	130	13	2	0	26	399	406	17
4	-2	15	188	178	18	2	-2	17	152	179	7	2	0	19	790	749	11	3	-1	22	437	427	19	1	1	26	500	500	14
0	-1	15	0	44	1	3	-2	17	235	232	14	3	0	19	472	479	11	0	0	22	308	287	16	2	1	26	26	57	26
1	-1	15	160	160	7	0	-1	17	268	257	8	4	0	19	298	331	21	1	0	22	114	96	18	0	-1	27	344	327	13
2	-1	15	139	157	10	1	-1	17	0	53	1	0	1	19	438	409	14	2	0	22	254	242	24	1	-1	27	200	240	13
3	-1	15	0	21	1	2	-1	17	411	414	7	1	1	19	635	628	11	3	0	22	69	15	69	1	0	27	0	21	1
4	-1	15	77	67	22	3	-1	17	177	183	10	2	1	19	106	134	22	1	1	22	353	355	10	2	0	27	183	228	39
1	0	15	14	43	14	4	-1	17	250	251	16	3	1	19	50	92	49	2	1	22	118	130	21	0	1	27	351	327	25
2	0	15	105	78	13	1	0	17	406	404	8	4	1	19	0	48	1	3	1	22	442	428	13	1	1	27	240	241	51
3	0	15	315	315	9	2	0	17	100	87	15	1	2	19	104	108	13	0	2	22	152	165	20	0	0	28	694	638	17
4	0	15	189	173	19	3	0	17	474	483	10	2	2	19	345	365	12	1	2	22	220	220	10	1	0	28	168	176	23

```
data_whelanite

_audit_creation_method            SHELXL-97
_chemical_name_systematic
;
 ?
;
_chemical_name_common             ?
_chemical_melting_point           ?
_chemical_formula_moiety          ?
_chemical_formula_sum
 'Ca6 Cu1.86 O26 Si6'
_chemical_formula_weight          943.20

loop_
 _atom_type_symbol
 _atom_type_description
 _atom_type_scat_dispersion_real
 _atom_type_scat_dispersion_imag
 _atom_type_scat_source
 'Cu'  'Cu'   0.3201   1.2651
 'International Tables Vol C Tables 4.2.6.8 and 6.1.1.4'
 'Ca'  'Ca'   0.2262   0.3064
 'International Tables Vol C Tables 4.2.6.8 and 6.1.1.4'
 'Si'  'Si'   0.0817   0.0704
 'International Tables Vol C Tables 4.2.6.8 and 6.1.1.4'
 'O'  'O'   0.0106   0.0060
 'International Tables Vol C Tables 4.2.6.8 and 6.1.1.4'

_symmetry_cell_setting            ?
_symmetry_space_group_name_H-M    Pn2n

loop_
 _symmetry_equiv_pos_as_xyz
 'x, y, z'
 'x+1/2, y+1/2, -z+1/2'
 '-x+1/2, y+1/2, z+1/2'
 '-x, y, -z'

_cell_length_a                    5.6551(4)
_cell_length_b                    3.683(3)
_cell_length_c                    27.1372(7)
_cell_angle_alpha                 90.00
_cell_angle_beta                  90.00
_cell_angle_gamma                 90.00
_cell_volume                      565.3(5)
_cell_formula_units_Z             1
_cell_measurement_temperature     293(2)
_cell_measurement_reflns_used     ?
_cell_measurement_theta_min       ?
_cell_measurement_theta_max       ?

_exptl_crystal_description        ?
_exptl_crystal_colour             ?
_exptl_crystal_size_max           0.15
```

```
_exptl_crystal_size_mid           0.05
_exptl_crystal_size_min           0.00
_exptl_crystal_density_meas       ?
_exptl_crystal_density_diffrn     2.771
_exptl_crystal_density_method     'not measured'
_exptl_crystal_F_000              466
_exptl_absorpt_coefficient_mu     3.552
_exptl_absorpt_correction_type    ?
_exptl_absorpt_correction_T_min   0.6178
_exptl_absorpt_correction_T_max   0.9965
_exptl_absorpt_process_details    ?

_exptl_special_details
;
 ?
;

_diffrn_ambient_temperature       293(2)
_diffrn_radiation_wavelength      0.71075
_diffrn_radiation_type            MoK\a
_diffrn_radiation_source          'fine-focus sealed tube'
_diffrn_radiation_monochromator   graphite
_diffrn_measurement_device_type   ?
_diffrn_measurement_method        ?
_diffrn_detector_area_resol_mean  ?
_diffrn_standards_number          ?
_diffrn_standards_interval_count  ?
_diffrn_standards_interval_time   ?
_diffrn_standards_decay_%         ?
_diffrn_reflns_number             3135
_diffrn_reflns_av_R_equivalents   0.0756
_diffrn_reflns_av_sigmaI/netI     0.0551
_diffrn_reflns_limit_h_min        -6
_diffrn_reflns_limit_h_max        6
_diffrn_reflns_limit_k_min        -3
_diffrn_reflns_limit_k_max        3
_diffrn_reflns_limit_l_min        -29
_diffrn_reflns_limit_l_max        29
_diffrn_reflns_theta_min          3.00
_diffrn_reflns_theta_max          22.44
_reflns_number_total              705
_reflns_number_gt                 567
_reflns_threshold_expression      >2sigma(I)

_computing_data_collection        ?
_computing_cell_refinement        ?
_computing_data_reduction         ?
_computing_structure_solution     'SHELXS-97 (Sheldrick, 1990)'
_computing_structure_refinement   'SHELXL-97 (Sheldrick, 1997)'
_computing_molecular_graphics     ?
_computing_publication_material   ?

_refine_special_details
;
 Refinement of F^2^ against ALL reflections.  The weighted R-factor wR and
```

```
 goodness of fit S are based on F^2^, conventional R-factors R are based
 on F, with F set to zero for negative F^2^. The threshold expression of
 F^2^ > 2sigma(F^2^) is used only for calculating R-factors(gt) etc. and is
 not relevant to the choice of reflections for refinement.  R-factors based
 on F^2^ are statistically about twice as large as those based on F, and R-
 factors based on ALL data will be even larger.
;

_refine_ls_structure_factor_coef  Fsqd
_refine_ls_matrix_type            full
_refine_ls_weighting_scheme       calc
_refine_ls_weighting_details
 'calc w=1/[\s^2^(Fo^2^)+(0.0339P)^2^+2.0112P] where P=(Fo^2^+2Fc^2^)/3'
_atom_sites_solution_primary      direct
_atom_sites_solution_secondary    difmap
_atom_sites_solution_hydrogens    geom
_refine_ls_hydrogen_treatment     mixed
_refine_ls_extinction_method      none
_refine_ls_extinction_coef        ?
_refine_ls_abs_structure_details
 'Flack H D (1983), Acta Cryst. A39, 876-881'
_refine_ls_abs_structure_Flack    0.37(12)
_refine_ls_number_reflns          705
_refine_ls_number_parameters      89
_refine_ls_number_restraints      2
_refine_ls_R_factor_all           0.0553
_refine_ls_R_factor_gt            0.0389
_refine_ls_wR_factor_ref          0.0898
_refine_ls_wR_factor_gt           0.0818
_refine_ls_goodness_of_fit_ref    1.069
_refine_ls_restrained_S_all       1.069
_refine_ls_shift/su_max           1.155
_refine_ls_shift/su_mean          0.134

loop_
 _atom_site_label
 _atom_site_type_symbol
 _atom_site_fract_x
 _atom_site_fract_y
 _atom_site_fract_z
 _atom_site_U_iso_or_equiv
 _atom_site_adp_type
 _atom_site_occupancy
 _atom_site_symmetry_multiplicity
 _atom_site_calc_flag
 _atom_site_refinement_flags
 _atom_site_disorder_assembly
 _atom_site_disorder_group
Cu Cu 0.0000 0.0000 0.0000 0.0161(6) Uani 0.920(7) 2 d SP . .
Ca1 Ca 0.5000 0.504(3) 0.0000 0.0166(6) Uani 1 2 d S . .
Ca2 Ca 0.6498(2) 0.999(2) 0.78612(5) 0.0121(5) Uani 1 1 d . . .
Si1A Si 0.650(2) 0.097(4) 0.6730(5) 0.0100(8) Uiso 0.50 1 d PD . .
Si1B Si 0.652(2) 0.932(4) 0.6733(4) 0.0100(8) Uiso 0.50 1 d PD . .
Si2 Si 0.8015(7) 0.514(4) 0.59994(14) 0.0128(11) Uiso 0.50 1 d P . .
O1 O 0.3767(8) 0.501(5) 0.79316(17) 0.0124(11) Uani 1 1 d . . .
```

```
O2 O 0.9147(8) 0.498(5) 0.79607(18) 0.0165(12) Uani 1 1 d . . .
O3 O 0.6983(8) 0.009(5) 0.03921(17) 0.0178(13) Uani 1 1 d . . .
O4 O 0.3914(13) 0.007(6) 0.1224(2) 0.051(2) Uani 1 1 d . . .
O5 O 0.1627(13) 0.668(3) 0.0440(3) 0.039(2) Uani 1 1 d . . .
O6A O 0.664(4) 0.843(7) 0.6234(8) 0.015(2) Uiso 0.50 1 d P . .
O6B O 0.668(4) 0.132(6) 0.6184(8) 0.015(2) Uiso 0.50 1 d P . .
O7 O 0.6448(15) 0.511(5) 0.6515(3) 0.013(2) Uiso 0.50 1 d PD . .

loop_
 _atom_site_aniso_label
 _atom_site_aniso_U_11
 _atom_site_aniso_U_22
 _atom_site_aniso_U_33
 _atom_site_aniso_U_23
 _atom_site_aniso_U_13
 _atom_site_aniso_U_12
Cu 0.0084(8) 0.0238(9) 0.0160(9) 0.000 0.0012(6) 0.000
Ca1 0.0145(11) 0.0161(13) 0.0192(13) 0.000 -0.0009(10) 0.000
Ca2 0.0111(8) 0.0085(9) 0.0165(9) -0.007(3) -0.0005(7) -0.003(3)
O1 0.012(2) 0.014(3) 0.011(3) 0.006(9) 0.002(2) 0.005(9)
O2 0.011(2) 0.015(3) 0.024(3) 0.005(12) 0.002(2) -0.002(9)
O3 0.015(3) 0.021(3) 0.018(3) 0.004(10) 0.002(2) 0.001(8)
O4 0.076(5) 0.054(5) 0.024(4) -0.017(12) -0.007(3) 0.002(14)
O5 0.020(4) 0.058(5) 0.039(5) 0.017(4) -0.002(4) 0.004(4)

_geom_special_details
;
 All esds (except the esd in the dihedral angle between two l.s. planes)
 are estimated using the full covariance matrix.  The cell esds are taken
 into account individually in the estimation of esds in distances, angles
 and torsion angles; correlations between esds in cell parameters are only
 used when they are defined by crystal symmetry.  An approximate (isotropic)
 treatment of cell esds is used for estimating esds involving l.s. planes.
;

loop_
 _geom_bond_atom_site_label_1
 _geom_bond_atom_site_label_2
 _geom_bond_distance
 _geom_bond_site_symmetry_2
 _geom_bond_publ_flag
Cu O5 1.941(9) 4_545 ?
Cu O5 1.941(9) 1_545 ?
Cu O3 2.011(5) 4_655 ?
Cu O3 2.011(5) 1_455 ?
Cu O5 2.886(10) . ?
Cu O5 2.886(10) 4 ?
Ca1 O5 2.331(8) . ?
Ca1 O5 2.331(8) 4_655 ?
Ca1 O3 2.390(15) 4_655 ?
Ca1 O3 2.390(15) . ?
Ca1 O3 2.419(15) 1_565 ?
Ca1 O3 2.419(15) 4_665 ?
Ca2 O2 2.385(16) 1_565 ?
Ca2 O2 2.393(16) . ?
```

```
Ca2 O1 2.406(13) . ?
Ca2 O1 2.417(14) 1_565 ?
Ca2 O4 2.495(7) 4_666 ?
Ca2 O1 2.505(5) 2_556 ?
Ca2 O2 2.597(5) 2_456 ?
Si1A O6B 1.49(3) . ?
Si1A O2 1.614(14) 2_446 ?
Si1A O1 1.616(14) 2_546 ?
Si1A O7 1.634(14) . ?
Si1A O6A 1.64(3) 1_545 ?
Si1A O7 2.235(17) 1_545 ?
Si1B O6A 1.39(3) . ?
Si1B O1 1.583(14) 2_556 ?
Si1B O2 1.598(13) 2_456 ?
Si1B O7 1.660(15) . ?
Si1B O6B 1.66(3) 1_565 ?
Si1B O7 2.214(17) 1_565 ?
Si2 O6A 1.57(3) . ?
Si2 O3 1.648(6) 3_655 ?
Si2 O7 1.656(10) . ?
Si2 O6B 1.68(2) . ?
Si2 O4 1.840(8) 3_655 ?
O1 Si1B 1.583(14) 2_446 ?
O1 Si1A 1.616(14) 2_456 ?
O1 Ca2 2.417(14) 1_545 ?
O1 Ca2 2.505(5) 2_446 ?
O2 Si1B 1.598(13) 2_546 ?
O2 Si1A 1.614(14) 2_556 ?
O2 Ca2 2.385(16) 1_545 ?
O2 Ca2 2.597(5) 2_546 ?
O3 Si2 1.648(6) 3_644 ?
O3 Cu 2.011(5) 1_655 ?
O3 Ca1 2.419(15) 1_545 ?
O4 Si2 1.840(8) 3_644 ?
O4 Ca2 2.495(7) 4_646 ?
O5 Cu 1.941(9) 1_565 ?
O6A O6B 1.072(12) 1_565 ?
O6A O7 1.45(3) . ?
O6A Si1A 1.64(3) 1_565 ?
O6A Cu 3.70(2) 2 ?
O6B O6A 1.072(12) 1_545 ?
O6B Si1B 1.66(3) 1_545 ?
O6B O7 1.67(3) . ?
O6B Cu 3.61(2) 2 ?
O6B Cu 4.08(2) 2_545 ?
O7 Si1B 2.214(17) 1_545 ?
O7 Si1A 2.235(16) 1_565 ?

loop_
 _geom_angle_atom_site_label_1
 _geom_angle_atom_site_label_2
 _geom_angle_atom_site_label_3
 _geom_angle
 _geom_angle_site_symmetry_1
 _geom_angle_site_symmetry_3
```

```
 _geom_angle_publ_flag
O5 Cu O5 101.9(6) 4_545 1_545 ?
O5 Cu O3 95.0(4) 4_545 4_655 ?
O5 Cu O3 86.2(4) 1_545 4_655 ?
O5 Cu O3 86.2(4) 4_545 1_455 ?
O5 Cu O3 95.0(4) 1_545 1_455 ?
O3 Cu O3 178.2(10) 4_655 1_455 ?
O5 Cu O5 160.5(3) 4_545 . ?
O5 Cu O5 97.5(3) 1_545 . ?
O3 Cu O5 86.3(4) 4_655 . ?
O3 Cu O5 92.2(5) 1_455 . ?
O5 Cu O5 97.5(3) 4_545 4 ?
O5 Cu O5 160.5(3) 1_545 4 ?
O3 Cu O5 92.2(5) 4_655 4 ?
O3 Cu O5 86.3(4) 1_455 4 ?
O5 Cu O5 63.0(3) . 4 ?
O5 Cu Si2 106.2(3) 4_545 3_544 ?
O5 Cu Si2 75.0(3) 1_545 3_544 ?
O3 Cu Si2 154.05(16) 4_655 3_544 ?
O3 Cu Si2 25.89(16) 1_455 3_544 ?
O5 Cu Si2 78.8(3) . 3_544 ?
O5 Cu Si2 99.6(3) 4 3_544 ?
O5 Cu Si2 75.0(3) 4_545 2_445 ?
O5 Cu Si2 106.2(3) 1_545 2_445 ?
O3 Cu Si2 25.89(16) 4_655 2_445 ?
O3 Cu Si2 154.05(16) 1_455 2_445 ?
O5 Cu Si2 99.6(3) . 2_445 ?
O5 Cu Si2 78.8(3) 4 2_445 ?
Si2 Cu Si2 178.2(6) 3_544 2_445 ?
O5 Cu Ca1 42.3(2) 4_545 1_445 ?
O5 Cu Ca1 93.2(3) 1_545 1_445 ?
O3 Cu Ca1 136.1(4) 4_655 1_445 ?
O3 Cu Ca1 45.3(4) 1_455 1_445 ?
O5 Cu Ca1 136.95(19) . 1_445 ?
O5 Cu Ca1 101.3(2) 4 1_445 ?
Si2 Cu Ca1 64.01(19) 3_544 1_445 ?
Si2 Cu Ca1 117.11(18) 2_445 1_445 ?
O5 Cu Ca1 93.2(3) 4_545 1_545 ?
O5 Cu Ca1 42.3(2) 1_545 1_545 ?
O3 Cu Ca1 45.3(4) 4_655 1_545 ?
O3 Cu Ca1 136.1(4) 1_455 1_545 ?
O5 Cu Ca1 101.3(2) . 1_545 ?
O5 Cu Ca1 136.95(19) 4 1_545 ?
Si2 Cu Ca1 117.11(18) 3_544 1_545 ?
Si2 Cu Ca1 64.01(19) 2_445 1_545 ?
Ca1 Cu Ca1 114.2(3) 1_445 1_545 ?
O5 Cu Ca1 87.1(3) 4_545 1_455 ?
O5 Cu Ca1 137.9(2) 1_545 1_455 ?
O3 Cu Ca1 134.5(4) 4_655 1_455 ?
O3 Cu Ca1 44.1(4) 1_455 1_455 ?
O5 Cu Ca1 78.4(2) . 1_455 ?
O5 Cu Ca1 42.75(18) 4 1_455 ?
Si2 Cu Ca1 63.01(19) 3_544 1_455 ?
Si2 Cu Ca1 115.86(18) 2_445 1_455 ?
Ca1 Cu Ca1 66.16(5) 1_445 1_455 ?
```

```
Ca1 Cu Ca1 179.6(3) 1_545 1_455 ?
O5 Cu Ca1 137.9(2) 4_545 . ?
O5 Cu Ca1 87.1(3) 1_545 . ?
O3 Cu Ca1 44.1(4) 4_655 . ?
O3 Cu Ca1 134.5(4) 1_455 . ?
O5 Cu Ca1 42.75(18) . . ?
O5 Cu Ca1 78.4(2) 4 . ?
Si2 Cu Ca1 115.86(18) 3_544 . ?
Si2 Cu Ca1 63.01(19) 2_445 . ?
Ca1 Cu Ca1 179.6(3) 1_445 . ?
Ca1 Cu Ca1 66.16(5) 1_545 . ?
Ca1 Cu Ca1 113.5(3) 1_455 . ?
O5 Ca1 O5 149.8(6) . 4_655 ?
O5 Ca1 O3 92.4(3) . 4_655 ?
O5 Ca1 O3 110.8(3) 4_655 4_655 ?
O5 Ca1 O3 110.8(3) . . ?
O5 Ca1 O3 92.4(3) 4_655 . ?
O3 Ca1 O3 80.6(6) 4_655 . ?
O5 Ca1 O3 87.4(4) . 1_565 ?
O5 Ca1 O3 69.3(3) 4_655 1_565 ?
O3 Ca1 O3 179.4(6) 4_655 1_565 ?
O3 Ca1 O3 99.98(18) . 1_565 ?
O5 Ca1 O3 69.3(3) . 4_665 ?
O5 Ca1 O3 87.4(4) 4_655 4_665 ?
O3 Ca1 O3 99.98(18) 4_655 4_665 ?
O3 Ca1 O3 179.4(6) . 4_665 ?
O3 Ca1 O3 79.5(6) 1_565 4_665 ?
O5 Ca1 Cu 123.1(4) . 1_665 ?
O5 Ca1 Cu 34.1(2) 4_655 1_665 ?
O3 Ca1 Cu 143.91(16) 4_655 1_665 ?
O3 Ca1 Cu 91.2(2) . 1_665 ?
O3 Ca1 Cu 36.20(14) 1_565 1_665 ?
O3 Ca1 Cu 88.4(3) 4_665 1_665 ?
O5 Ca1 Cu 34.1(2) . 1_565 ?
O5 Ca1 Cu 123.1(4) 4_655 1_565 ?
O3 Ca1 Cu 91.2(2) 4_655 1_565 ?
O3 Ca1 Cu 143.91(16) . 1_565 ?
O3 Ca1 Cu 88.4(3) 1_565 1_565 ?
O3 Ca1 Cu 36.20(14) 4_665 1_565 ?
Cu Ca1 Cu 114.2(3) 1_665 1_565 ?
O5 Ca1 Cu 57.2(2) . . ?
O5 Ca1 Cu 145.8(3) 4_655 . ?
O3 Ca1 Cu 35.84(13) 4_655 . ?
O3 Ca1 Cu 88.5(3) . . ?
O3 Ca1 Cu 144.05(17) 1_565 . ?
O3 Ca1 Cu 92.0(2) 4_665 . ?
Cu Ca1 Cu 179.6(3) 1_665 . ?
Cu Ca1 Cu 66.16(5) 1_565 . ?
O5 Ca1 Cu 145.8(3) . 1_655 ?
O5 Ca1 Cu 57.2(2) 4_655 1_655 ?
O3 Ca1 Cu 88.5(3) 4_655 1_655 ?
O3 Ca1 Cu 35.84(13) . 1_655 ?
O3 Ca1 Cu 92.0(2) 1_565 1_655 ?
O3 Ca1 Cu 144.05(17) 4_665 1_655 ?
Cu Ca1 Cu 66.16(5) 1_665 1_655 ?
```

```
Cu Ca1 Cu 179.6(3) 1_565 1_655 ?
Cu Ca1 Cu 113.5(3) . 1_655 ?
O5 Ca1 Si2 105.8(2) . 2_445 ?
O5 Ca1 Si2 90.0(2) 4_655 2_445 ?
O3 Ca1 Si2 25.5(3) 4_655 2_445 ?
O3 Ca1 Si2 96.0(5) . 2_445 ?
O3 Ca1 Si2 154.2(3) 1_565 2_445 ?
O3 Ca1 Si2 84.6(3) 4_665 2_445 ?
Cu Ca1 Si2 123.91(10) 1_665 2_445 ?
Cu Ca1 Si2 90.61(15) 1_565 2_445 ?
Cu Ca1 Si2 55.97(15) . 2_445 ?
Cu Ca1 Si2 89.2(2) 1_655 2_445 ?
O5 Ca1 Si2 90.0(2) . 3_644 ?
O5 Ca1 Si2 105.8(2) 4_655 3_644 ?
O3 Ca1 Si2 96.0(5) 4_655 3_644 ?
O3 Ca1 Si2 25.5(3) . 3_644 ?
O3 Ca1 Si2 84.6(3) 1_565 3_644 ?
O3 Ca1 Si2 154.2(3) 4_665 3_644 ?
Cu Ca1 Si2 90.61(15) 1_665 3_644 ?
Cu Ca1 Si2 123.91(10) 1_565 3_644 ?
Cu Ca1 Si2 89.2(2) . 3_644 ?
Cu Ca1 Si2 55.97(15) 1_655 3_644 ?
Si2 Ca1 Si2 116.9(6) 2_445 3_644 ?
O2 Ca2 O2 100.86(18) 1_565 . ?
O2 Ca2 O1 168.91(18) 1_565 . ?
O2 Ca2 O1 78.7(4) . . ?
O2 Ca2 O1 78.7(4) 1_565 1_565 ?
O2 Ca2 O1 168.95(17) . 1_565 ?
O1 Ca2 O1 99.60(17) . 1_565 ?
O2 Ca2 O4 86.4(5) 1_565 4_666 ?
O2 Ca2 O4 87.4(5) . 4_666 ?
O1 Ca2 O4 82.5(5) . 4_666 ?
O1 Ca2 O4 81.5(5) 1_565 4_666 ?
O2 Ca2 O1 76.9(4) 1_565 2_556 ?
O2 Ca2 O1 77.2(4) . 2_556 ?
O1 Ca2 O1 113.5(5) . 2_556 ?
O1 Ca2 O1 113.1(5) 1_565 2_556 ?
O4 Ca2 O1 154.5(2) 4_666 2_556 ?
O2 Ca2 O2 114.9(6) 1_565 2_456 ?
O2 Ca2 O2 114.6(6) . 2_456 ?
O1 Ca2 O2 74.8(4) . 2_456 ?
O1 Ca2 O2 75.1(4) 1_565 2_456 ?
O4 Ca2 O2 143.8(2) 4_666 2_456 ?
O1 Ca2 O2 61.61(14) 2_556 2_456 ?
O2 Ca2 Si1B 99.9(3) 1_565 . ?
O2 Ca2 Si1B 92.7(3) . . ?
O1 Ca2 Si1B 91.2(3) . . ?
O1 Ca2 Si1B 98.3(3) 1_565 . ?
O4 Ca2 Si1B 173.5(5) 4_666 . ?
O1 Ca2 Si1B 30.9(3) 2_556 . ?
O2 Ca2 Si1B 31.3(3) 2_456 . ?
O2 Ca2 Si1A 91.3(3) 1_565 1_565 ?
O2 Ca2 Si1A 101.6(3) . 1_565 ?
O1 Ca2 Si1A 99.6(3) . 1_565 ?
O1 Ca2 Si1A 89.4(3) 1_565 1_565 ?
```

```
O4 Ca2 Si1A 170.9(6) 4_666 1_565 ?
O1 Ca2 Si1A 31.4(3) 2_556 1_565 ?
O2 Ca2 Si1A 31.5(3) 2_456 1_565 ?
Si1B Ca2 Si1A 11.31(9) . 1_565 ?
O2 Ca2 Si1A 77.0(4) 1_565 2_556 ?
O2 Ca2 Si1A 25.9(4) . 2_556 ?
O1 Ca2 Si1A 100.2(3) . 2_556 ?
O1 Ca2 Si1A 147.6(3) 1_565 2_556 ?
O4 Ca2 Si1A 75.9(4) 4_666 2_556 ?
O1 Ca2 Si1A 81.7(3) 2_556 2_556 ?
O2 Ca2 Si1A 135.2(4) 2_456 2_556 ?
Si1B Ca2 Si1A 106.7(3) . 2_556 ?
Si1A Ca2 Si1A 112.1(4) 1_565 2_556 ?
O2 Ca2 Si1A 145.7(3) 1_565 2_456 ?
O2 Ca2 Si1A 98.5(4) . 2_456 ?
O1 Ca2 Si1A 26.1(3) . 2_456 ?
O1 Ca2 Si1A 77.0(4) 1_565 2_456 ?
O4 Ca2 Si1A 66.4(4) 4_666 2_456 ?
O1 Ca2 Si1A 135.4(3) 2_556 2_456 ?
O2 Ca2 Si1A 81.5(3) 2_456 2_456 ?
Si1B Ca2 Si1A 107.2(3) . 2_456 ?
Si1A Ca2 Si1A 112.1(4) 1_565 2_456 ?
Si1A Ca2 Si1A 113.5(4) 2_556 2_456 ?
O2 Ca2 Si1B 97.0(4) 1_565 2_456 ?
O2 Ca2 Si1B 147.0(3) . 2_456 ?
O1 Ca2 Si1B 78.5(4) . 2_456 ?
O1 Ca2 Si1B 24.7(3) 1_565 2_456 ?
O4 Ca2 Si1B 66.2(4) 4_666 2_456 ?
O1 Ca2 Si1B 134.2(3) 2_556 2_456 ?
O2 Ca2 Si1B 81.7(3) 2_456 2_456 ?
Si1B Ca2 Si1B 111.3(3) . 2_456 ?
Si1A Ca2 Si1B 105.4(3) 1_565 2_456 ?
Si1A Ca2 Si1B 141.99(16) 2_556 2_456 ?
Si1A Ca2 Si1B 53.82(9) 2_456 2_456 ?
Si1B Si1A O6B 96(2) 1_545 . ?
Si1B Si1A O2 78(2) 1_545 2_446 ?
O6B Si1A O2 126.3(12) . 2_446 ?
Si1B Si1A O1 76(2) 1_545 2_546 ?
O6B Si1A O1 122.0(12) . 2_546 ?
O2 Si1A O1 108.0(8) 2_446 2_546 ?
Si1B Si1A O7 160(3) 1_545 . ?
O6B Si1A O7 64.2(11) . . ?
O2 Si1A O7 112.4(11) 2_446 . ?
O1 Si1A O7 114.8(10) 2_546 . ?
Si1B Si1A O6A 56(2) 1_545 1_545 ?
O6B Si1A O6A 39.7(6) . 1_545 ?
O2 Si1A O6A 109.8(12) 2_446 1_545 ?
O1 Si1A O6A 107.7(12) 2_546 1_545 ?
O7 Si1A O6A 103.8(12) . 1_545 ?
Si1B Si1A O7 16(2) 1_545 1_545 ?
O6B Si1A O7 79.9(10) . 1_545 ?
O2 Si1A O7 84.7(8) 2_446 1_545 ?
O1 Si1A O7 87.1(8) 2_546 1_545 ?
O7 Si1A O7 143.9(9) . 1_545 ?
O6A Si1A O7 40.3(9) 1_545 1_545 ?
```

```
Si1B Si1A Si2 126(2) 1_545 . ?
O6B Si1A Si2 35.4(9) . . ?
O2 Si1A Si2 141.8(9) 2_446 . ?
O1 Si1A Si2 107.1(7) 2_546 . ?
O7 Si1A Si2 36.6(5) . . ?
O6A Si1A Si2 72.6(10) 1_545 . ?
O7 Si1A Si2 111.6(6) 1_545 . ?
Si1B Si1A Ca2 83(2) 1_545 1_545 ?
O6B Si1A Ca2 175.8(12) . 1_545 ?
O2 Si1A Ca2 57.1(4) 2_446 1_545 ?
O1 Si1A Ca2 53.9(4) 2_546 1_545 ?
O7 Si1A Ca2 117.6(7) . 1_545 ?
O6A Si1A Ca2 138.5(10) 1_545 1_545 ?
O7 Si1A Ca2 98.5(4) 1_545 1_545 ?
Si2 Si1A Ca2 144.1(5) . 1_545 ?
Si1B Si1A Ca2 117(3) 1_545 2_446 ?
O6B Si1A Ca2 110.2(11) . 2_446 ?
O2 Si1A Ca2 40.4(8) 2_446 2_446 ?
O1 Si1A Ca2 124.9(7) 2_546 2_446 ?
O7 Si1A Ca2 72.1(6) . 2_446 ?
O6A Si1A Ca2 124.1(10) 1_545 2_446 ?
O7 Si1A Ca2 119.9(5) 1_545 2_446 ?
Si2 Si1A Ca2 105.2(4) . 2_446 ?
Ca2 Si1A Ca2 74.0(3) 1_545 2_446 ?
Si1B Si1A Ca2 115(3) 1_545 2_546 ?
O6B Si1A Ca2 103.4(10) . 2_546 ?
O2 Si1A Ca2 128.1(7) 2_446 2_546 ?
O1 Si1A Ca2 41.0(7) 2_546 2_546 ?
O7 Si1A Ca2 73.9(5) . 2_546 ?
O6A Si1A Ca2 118.5(10) 1_545 2_546 ?
O7 Si1A Ca2 121.3(6) 1_545 2_546 ?
Si2 Si1A Ca2 73.8(3) . 2_546 ?
Ca2 Si1A Ca2 74.0(3) 1_545 2_546 ?
Ca2 Si1A Ca2 113.5(4) 2_446 2_546 ?
Si1A Si1B O6A 103(3) 1_565 . ?
Si1A Si1B O1 82(2) 1_565 2_556 ?
O6A Si1B O1 123.9(13) . 2_556 ?
Si1A Si1B O2 81(2) 1_565 2_456 ?
O6A Si1B O2 125.6(13) . 2_456 ?
O1 Si1B O2 110.5(7) 2_556 2_456 ?
Si1A Si1B O7 158(3) 1_565 . ?
O6A Si1B O7 55.7(12) . . ?
O1 Si1B O7 112.1(10) 2_556 . ?
O2 Si1B O7 107.9(11) 2_456 . ?
Si1A Si1B O6B 63(2) 1_565 1_565 ?
O6A Si1B O6B 39.8(6) . 1_565 ?
O1 Si1B O6B 113.6(11) 2_556 1_565 ?
O2 Si1B O6B 116.2(11) 2_456 1_565 ?
O7 Si1B O6B 95.5(11) . 1_565 ?
Si1A Si1B O7 15(2) 1_565 1_565 ?
O6A Si1B O7 88.1(12) . 1_565 ?
O1 Si1B O7 90.7(9) 2_556 1_565 ?
O2 Si1B O7 88.6(9) 2_456 1_565 ?
O7 Si1B O7 143.5(9) . 1_565 ?
O6B Si1B O7 48.3(9) 1_565 1_565 ?
```

```
Si1A Si1B Si2 125(2) 1_565 . ?
O6A Si1B Si2 28.4(10) . . ?
O1 Si1B Si2 105.7(7) 2_556 . ?
O2 Si1B Si2 138.2(9) 2_456 . ?
O7 Si1B Si2 36.8(5) . . ?
O6B Si1B Si2 64.4(9) 1_565 . ?
O7 Si1B Si2 111.3(6) 1_565 . ?
Si1A Si1B Ca2 86(2) 1_565 . ?
O6A Si1B Ca2 170.8(12) . . ?
O1 Si1B Ca2 54.4(4) 2_556 . ?
O2 Si1B Ca2 57.7(4) 2_456 . ?
O7 Si1B Ca2 115.5(6) . . ?
O6B Si1B Ca2 148.9(10) 1_565 . ?
O7 Si1B Ca2 100.9(4) 1_565 . ?
Si2 Si1B Ca2 142.7(5) . . ?
Si1A Si1B Ca2 119(3) 1_565 2_546 ?
O6A Si1B Ca2 99.5(11) . 2_546 ?
O1 Si1B Ca2 39.6(7) 2_556 2_546 ?
O2 Si1B Ca2 126.6(7) 2_456 2_546 ?
O7 Si1B Ca2 72.6(5) . 2_546 ?
O6B Si1B Ca2 116.9(9) 1_565 2_546 ?
O7 Si1B Ca2 123.4(5) 1_565 2_546 ?
Si2 Si1B Ca2 73.1(3) . 2_546 ?
Ca2 Si1B Ca2 73.7(3) . 2_546 ?
Si1A Si1B Ca2 117(3) 1_565 2_446 ?
O6A Si1B Ca2 104.1(12) . 2_446 ?
O1 Si1B Ca2 123.6(7) 2_556 2_446 ?
O2 Si1B Ca2 37.8(8) 2_456 2_446 ?
O7 Si1B Ca2 70.2(5) . 2_446 ?
O6B Si1B Ca2 122.4(9) 1_565 2_446 ?
O7 Si1B Ca2 121.1(5) 1_565 2_446 ?
Si2 Si1B Ca2 103.6(5) . 2_446 ?
Ca2 Si1B Ca2 73.4(3) . 2_446 ?
Ca2 Si1B Ca2 111.2(4) 2_546 2_446 ?
O6A Si2 O3 114.4(11) . 3_655 ?
O6A Si2 O7 53.1(10) . . ?
O3 Si2 O7 147.6(4) 3_655 . ?
O6A Si2 O6B 107.7(5) . . ?
O3 Si2 O6B 106.8(11) 3_655 . ?
O7 Si2 O6B 60.0(10) . . ?
O6A Si2 O4 110.0(11) . 3_655 ?
O3 Si2 O4 109.3(3) 3_655 3_655 ?
O7 Si2 O4 103.1(4) . 3_655 ?
O6B Si2 O4 108.4(11) . 3_655 ?
O6A Si2 Si1A 89.1(9) . . ?
O3 Si2 Si1A 137.8(9) 3_655 . ?
O7 Si2 Si1A 36.0(7) . . ?
O6B Si2 Si1A 31.0(8) . . ?
O4 Si2 Si1A 92.9(6) 3_655 . ?
O6A Si2 Si1B 24.9(8) . . ?
O3 Si2 Si1B 139.2(9) 3_655 . ?
O7 Si2 Si1B 36.9(6) . . ?
O6B Si2 Si1B 96.9(8) . . ?
O4 Si2 Si1B 93.4(6) 3_655 . ?
Si1A Si2 Si1B 70.88(15) . . ?
```

```
O6A Si2 Cu 95.3(9) . 2 ?
O3 Si2 Cu 32.19(19) 3_655 2 ?
O7 Si2 Cu 115.5(3) . 2 ?
O6B Si2 Cu 89.9(8) . 2 ?
O4 Si2 Cu 141.4(3) 3_655 2 ?
Si1A Si2 Cu 116.8(4) . 2 ?
Si1B Si2 Cu 118.4(4) . 2 ?
O6A Si2 Ca1 94.3(10) . 2 ?
O3 Si2 Ca1 38.6(6) 3_655 2 ?
O7 Si2 Ca1 147.5(10) . 2 ?
O6B Si2 Ca1 145.3(9) . 2 ?
O4 Si2 Ca1 87.7(5) 3_655 2 ?
Si1A Si2 Ca1 176.0(6) . 2 ?
Si1B Si2 Ca1 113.0(6) . 2 ?
Cu Si2 Ca1 61.02(12) 2 2 ?
O6A Si2 Ca1 152.7(9) . 2_545 ?
O3 Si2 Ca1 38.3(6) 3_655 2_545 ?
O7 Si2 Ca1 145.7(10) . 2_545 ?
O6B Si2 Ca1 85.7(9) . 2_545 ?
O4 Si2 Ca1 86.9(5) 3_655 2_545 ?
Si1A Si2 Ca1 111.9(6) . 2_545 ?
Si1B Si2 Ca1 177.2(6) . 2_545 ?
Cu Si2 Ca1 60.27(12) 2 2_545 ?
Ca1 Si2 Ca1 64.21(8) 2 2_545 ?
Si1B O1 Si1A 21.85(19) 2_446 2_456 ?
Si1B O1 Ca2 133.2(10) 2_446 . ?
Si1A O1 Ca2 112.9(10) 2_456 . ?
Si1B O1 Ca2 115.7(10) 2_446 1_545 ?
Si1A O1 Ca2 135.9(9) 2_456 1_545 ?
Ca2 O1 Ca2 99.60(17) . 1_545 ?
Si1B O1 Ca2 94.7(5) 2_446 2_446 ?
Si1A O1 Ca2 94.7(5) 2_456 2_446 ?
Ca2 O1 Ca2 105.2(4) . 2_446 ?
Ca2 O1 Ca2 104.9(4) 1_545 2_446 ?
Si1B O2 Si1A 21.79(19) 2_546 2_556 ?
Si1B O2 Ca2 118.0(11) 2_546 1_545 ?
Si1A O2 Ca2 138.6(10) 2_556 1_545 ?
Si1B O2 Ca2 134.6(11) 2_546 . ?
Si1A O2 Ca2 113.6(11) 2_556 . ?
Ca2 O2 Ca2 100.86(18) 1_545 . ?
Si1B O2 Ca2 91.0(5) 2_546 2_546 ?
Si1A O2 Ca2 91.4(5) 2_556 2_546 ?
Ca2 O2 Ca2 103.1(5) 1_545 2_546 ?
Ca2 O2 Ca2 102.8(5) . 2_546 ?
Si2 O3 Cu 121.9(3) 3_644 1_655 ?
Si2 O3 Ca1 115.9(8) 3_644 . ?
Cu O3 Ca1 100.1(4) 1_655 . ?
Si2 O3 Ca1 116.7(8) 3_644 1_545 ?
Cu O3 Ca1 98.5(5) 1_655 1_545 ?
Ca1 O3 Ca1 99.98(18) . 1_545 ?
Si2 O3 Cu 105.1(2) 3_644 . ?
Cu O3 Cu 132.95(19) 1_655 . ?
Ca1 O3 Cu 55.75(16) . . ?
Ca1 O3 Cu 55.38(15) 1_545 . ?
Si2 O4 Ca2 114.7(3) 3_644 4_646 ?
```

```
Si2 O4 Cu 104.4(3) 3_644 . ?
Ca2 O4 Cu 140.9(3) 4_646 . ?
Cu O5 Ca1 103.7(4) 1_565 . ?
Cu O5 Cu 97.5(3) 1_565 . ?
Ca1 O5 Cu 80.0(3) . . ?
O6B O6A Si1B 84(2) 1_565 . ?
O6B O6A O7 155(3) 1_565 . ?
Si1B O6A O7 71.5(12) . . ?
O6B O6A Si2 135(3) 1_565 . ?
Si1B O6A Si2 126.6(16) . . ?
O7 O6A Si2 66.3(11) . . ?
O6B O6A Si1A 63(2) 1_565 1_565 ?
Si1B O6A Si1A 21.2(6) . 1_565 ?
O7 O6A Si1A 92.6(13) . 1_565 ?
Si2 O6A Si1A 142.6(15) . 1_565 ?
O6B O6A Cu 103(2) 1_565 2 ?
Si1B O6A Cu 161.3(15) . 2 ?
O7 O6A Cu 99.7(12) . 2 ?
Si2 O6A Cu 59.6(7) . 2 ?
Si1A O6A Cu 157.7(12) 1_565 2 ?
O6A O6B Si1A 78(2) 1_545 . ?
O6A O6B Si1B 56(2) 1_545 1_545 ?
Si1A O6B Si1B 21.3(4) . 1_545 ?
O6A O6B O7 140(3) 1_545 . ?
Si1A O6B O7 62.1(9) . . ?
Si1B O6B O7 83.4(11) 1_545 . ?
O6A O6B Si2 152(3) 1_545 . ?
Si1A O6B Si2 113.6(14) . . ?
Si1B O6B Si2 131.5(14) 1_545 . ?
O7 O6B Si2 59.4(9) . . ?
O6A O6B Cu 119(2) 1_545 2 ?
Si1A O6B Cu 154.0(13) . 2 ?
Si1B O6B Cu 161.5(11) 1_545 2 ?
O7 O6B Cu 98.3(10) . 2 ?
Si2 O6B Cu 62.5(7) . 2 ?
O6A O6B Cu 62(2) 1_545 2_545 ?
Si1A O6B Cu 135.9(11) . 2_545 ?
Si1B O6B Cu 116.1(10) 1_545 2_545 ?
O7 O6B Cu 152.3(11) . 2_545 ?
Si2 O6B Cu 110.4(10) . 2_545 ?
Cu O6B Cu 56.8(3) 2 2_545 ?
O6A O7 Si1A 167.8(13) . . ?
O6A O7 Si2 60.6(11) . . ?
Si1A O7 Si2 107.4(11) . . ?
O6A O7 Si1B 52.8(12) . . ?
Si1A O7 Si1B 138.1(6) . . ?
Si2 O7 Si1B 106.3(11) . . ?
O6A O7 O6B 114.8(8) . . ?
Si1A O7 O6B 53.7(11) . . ?
Si2 O7 O6B 60.6(9) . . ?
Si1B O7 O6B 166.8(11) . . ?
O6A O7 Si1B 162.7(12) . 1_545 ?
Si1A O7 Si1B 5.4(7) . 1_545 ?
Si2 O7 Si1B 102.9(9) . 1_545 ?
Si1B O7 Si1B 143.5(9) . 1_545 ?
```

```
O6B O7 Si1B 48.3(9) . 1_545 ?
O6A O7 Si1A 47.1(11) . 1_565 ?
Si1A O7 Si1A 143.9(9) . 1_565 ?
Si2 O7 Si1A 102.0(9) . 1_565 ?
Si1B O7 Si1A 5.8(7) . 1_565 ?
O6B O7 Si1A 161.7(10) . 1_565 ?
Si1B O7 Si1A 149.3(5) 1_545 1_565 ?

_diffrn_measured_fraction_theta_max    0.988
_diffrn_reflns_theta_full              22.44
_diffrn_measured_fraction_theta_full   0.988
_refine_diff_density_max    0.993
_refine_diff_density_min   -0.431
_refine_diff_density_rms    0.135
```